Bridge Load Testing Versus Bridge Load Rating

Kentucky Transportation Center
College of Engineering, University of Kentucky Lexington, Kentucky

in cooperation with
Kentucky Transportation Cabinet
Commonwealth of Kentucky

Kentucky Transportation Center • University of Kentucky
176 Raymond Building • Lexington KY 40506 • 859.257.6898 • www.ktc.uky.edu

Bridge Load Testing Versus Bridge Load Rating

Abheetha Peiris, Ph.D.
Research Engineer

and

Issam E. Harik, Ph.D.
Professor of Civil Engineering

Kentucky Transportation Center
College of Engineering
University of Kentucky
Lexington, Kentucky

In Cooperation With
Kentucky Transportation Cabinet
Commonwealth of Kentucky

June 2019

1. Report No. KTC-19-16/SPR06-423-1F	2. Government Accession No.	3. Recipient's Catalog No	
4. **Title and Subtitle** Bridge Load Testing Versus Bridge Load Rating		5. **Report Date** June 2019	
		6. **Performing Organization Code**	
7. **Author(s):** Abheetha Peiris, Issam Harik		8. **Performing Organization Report No.** KTC-19-16/SPR06-423-1F	
9. **Performing Organization Name and Address** Kentucky Transportation Center College of Engineering University of Kentucky Lexington, KY 40506-0281		10. **Work Unit No. (TRAIS)**	
		11. **Contract or Grant No.** SPR 06-423	
12. **Sponsoring Agency Name and Address** Kentucky Transportation Cabinet State Office Building Frankfort, KY 40622		13. **Type of Report and Period Covered**	
		14. **Sponsoring Agency Code**	

15. Supplementary Notes
Prepared in cooperation with the Kentucky Transportation Cabinet

16. Abstract
The current method of load rating bridges according to AASHTO specifications can underestimate the capacity and behavior of bridges. Analytical equations do not account for the degree of rigidity of the supports, unintended composite action due to friction between girders and the slab, and other factors. Load testing of individual bridges can produce a load rating that much more accurately reflects the capacity of a non-composite bridge. However, current methods of load testing require significant time commitments to instrument a bridge profile to record data, rendering it impractical in many cases. But there are new commercially available strain gauges that greatly reduce the time required to instrument a location. This study evaluated the accuracy and efficiency of set up of the magnetic Sensormate QE-1010 strain gauge and reusable BDI ST350 strain gauge. Both gauge types were interfaced with wireless data transmission capabilities, tested in laboratories alongside the more traditional foil-type strain gauges, and deployed on two Kentucky bridges to test their overall efficacy. Although magnetic strain gauges performed well in the field and reduced installation time, due to the rugged requirements of field testing, they will not be considered for future deployments given the current status of the technology. Reusable strain gauges coupled with wireless transmitters balance rugged performance with short installation times. The field-tested bridges were load posted due to the load rating factor for several truck types being less than one. Field load tests revealed the load rating factor for strength was adequate for the KY 220 Bridge in Hardin County while the load rating for the KY 1068 Bridge in Lewis County could be increased by 68%.

17. **Key Words** bridge testing, load rating, load distribution, non-composite deck, steel girder		18. **Distribution Statement** Unlimited with approval of the Kentucky Transportation Cabinet	
19. **Security Classification (report)** Unclassified	20. Security Classification (this page) Unclassified	21. No. of Pages	19. **Security Classification (report)**

Executive Summary

The current method for load rating bridges — based on AASHTO specifications — can underestimate the capacity and behavior of bridges. Analytical equations do not account for the degree of rigidity in supports, unintended composite action due to friction between girders and the slab, and other factors. Load testing of individual bridges can produce a load rating that much more accurately reflects the capacity of a non-composite bridge. However, current methods of load testing require significant time commitments to instrument a bridge profile to record data, rendering it less feasible. New types of commercially available strain gauges, however, significantly reduce the time required to instrument a location.

This report discusses the load rating of two bridges using field load test data. Researchers evaluated two types of strain gauges in field load tests to determine how effectively they minimize deployment time while maintaining accuracy. Magnetic Sensormate QE-1010 strain gauges and reusable BDI ST350 strain gauges were outfitted with wireless data transmission capabilities for rapid field deployment. The goal was to determine if using these gauges would significantly reduce the amount of time required to load test a bridge. For bridges with characteristics such as unintended composite action or end fixity, this would increase the feasibility of load testing bridges, leading to a more favorable load rating. Compared to the theoretical load ratings, ratings based on load tests are expected to be more accurate.

Both gauge types were tested in the laboratory under flexural loads. Their readings were compared to those obtained from traditional foil-type strain gauges prior to their deployment on two bridges in Kentucky. Laboratory tests demonstrated the magnetic strain gauges and BDI reusable strain gauges are very accurate at low strains. At higher strains (i.e., more than 400 microstrain) the magnetic strain gauges slipped. The wireless data transmission capability of both systems made it possible to carry out data acquisition without being close to the gauges. This significantly reduced the amount of wiring typically associated with strain gauge data acquisition. While magnetic strain gauges performed well in the field and gauge installation time was reduced, due to the rugged requirements of field testing they will not be considered for future deployments given the current status of the technology. Reusable BDI strain gauges coupled with wireless transmitters balance rugged performance with short installation times.

Each bridge was load posted because the load rating factor for several truck types was less than one. Table E1 lists the AASHTO load rating and field load testing results for the KY 1068 and KY 220 bridges. Field load tests revealed the load rating factor for strength was adequate for the KY 220 Bridge in Hardin County, while the load rating for the KY 1068 Bridge in Lewis County could be increased by 68%.

Table E1 Load Rating Results

Bridge	Governing Truck Type	AASHTO Analytical Rating Factor	Load Test Rating Factor
KY 1068 – Lewis County	KY Type 3	0.48	0.70
KY 220 – Hardin County	KY Type 3	0.62	1.25

With the development of better, low-cost, wireless, and non-contact sensing technology, field load rating is now a more attainable option for evaluating bridge load ratings. In addition to accurately describing bridge behavior and highlighting unintended factors that may increase load ratings, the technology can also be used to diagnose structural deficiencies.

Table of Contents

List of Figures

List of Tables

Acknowledgements

1. Introduction

Accurately analyzing and predicting the load bearing capacity of bridges is critical for protecting the safety of the traveling public. In the United States, the National Bridge Inspection Standards (NBIS) require that all bridges on public roads be assigned a load rating. Bridge owners, typically state departments of transportation (DOTs), are responsible for the load ratings of these bridges based on the NBIS. Load ratings should be carried out pursuant to guidelines in the American Association of State Highway and Transportation Officials' (AASHTO) *Manual for Bridge Evaluation* (MBE) [1].

The MBE's theoretical approach has been used to load rate most bridges in the United States. According to the MBE, the objective of a load rating is to evaluate the safe live load carrying capacity of a bridge based on as-built construction plans and material properties while accounting for any structural damage. This is important because historically bridges have been designed using several different design truck and lane loads. Load ratings are expressed as a Rating Factor (RF) or in terms of a particular truck weight in tons. Two different ratings are carried out: (1) Inventory Rating and (2) Operating Rating. The Inventory Rating represents the live load that can traverse a bridge an indefinite number of times; the Operating Rating represents the maximum permissible live load that can move across a bridge safely. When a bridge of insufficient capacity is identified, truck loads are restricted by load posting.

The theoretical load rating calculated based on the MBE approach tends to be conservative due to many of the assumptions made in the calculation process. The live load distribution in longitudinal beams is one assumption evaluated based on recommendations in AASHTO's *Specifications for Highway Bridges* [2]. In addition, many bridges on secondary roads lack construction plans from which material and section properties can be discerned, requiring these properties to be estimated. As numerous studies [3-7] have shown, field testing bridges can provide more accurate and reliable information about their present condition.

Due to its inherent advantages, the MBE dedicates an entire chapter to guidelines for establishing load ratings using non-destructive load testing. The MBE identifies two types of load tests: (1) diagnostic tests and (2) proof tests.

While diagnostic load tests are carried out to determine certain response characteristics of a bridge, proof tests are used to evaluate a bridge's safe load carrying capacity. Load tests are categorized as static or dynamic. Both are typically used for diagnostic load tests, while static load tests are primarily used for proof load tests. Diagnostic load tests are typically used to measure load effects on a bridge and compare them with analytical models or theoretical calculations. Calibrated finite element models (FEM) can be developed based on diagnostic tests to predict bridge response to different loading scenarios. Proof load tests are more useful when a bridge cannot be analytically load rated (e.g., when material or section properties are unavailable and cannot be accurately determined).

The MBE [1] lists several factors that increase the live load capacity of a bridge and which can be evaluated through a load test, including:

1. Unintended composite action
2. Unintended continuity/fixity
3. Participation of secondary members
4. Portion of load carried by deck

All or most of these factors influence the live load capacity of non-composite steel girder bridges, as all these factors are neglected when a bridge is analytically load rated. Field load tests can also provide accurate load distribution factors for the main beams, which are otherwise based on conservative design load distribution factors. Field testing can also identify possible structural deficiencies and damages not observed during routine inspections.

However, load testing a bridge can take multiple days. This includes time for setting up equipment, conducting load testing, and data reduction and analysis. With advances in strain gauge and instrumentation technology, rapidly and efficiently load testing bridges is growing more feasible. New commercially available gauge types greatly reduce the time required to place sensors across a bridge, which is one of the most time-consuming exercises, thereby making field load tests a much faster and more feasible option for load rating of bridges. In this study, two types of gauges were tested to evaluate how much time they save when instrumenting a bridge for load testing; their accuracy was also assessed. Gauges were compared to traditional foil-type strain gauges with respect to their accuracy and time required to set up equipment. The report discusses the field load testing of two steel girder bridges with non-composite concrete decks in Kentucky using the novel strain gauges. It also provides details on the instrumentation calibration and use as well as the resulting load ratings.

2. Bridge Load Rating Through Load Testing

The MBE details three rating methods: Allowable Stress Rating (ASR), Load Factor Rating (LFR) and Load and Resistance Factor Rating (LRFR). Developed most recently, the LRFR provides a more uniform safety margin in terms of reliability, however, most state DOTs prefer LFD when load rating bridges designed using either allowable stress or a load factor-based design. Because the two bridges highlighted in this report are steel girder bridges built prior to implementation of LRFR, researchers carried out the load rating using LFR. An analytical load rating of a bridge should be carried out before doing any load testing. The MBE specifies the following equation to calculate the RF based on LFR [1]:

$$RF = \frac{C - A_1 D}{A_2 L (I + 1)} \qquad (1)$$

Where:

C = Capacity of the member

D = Dead load effect on the member

L = Live load effect on the member

I = Impact factor

A_1 = Factor for dead loads

A_2 = Factor for live loads

The factors A_1, A_2 vary depending on the level of rating performed — Inventory or Operating. The dead and live load effects used for analytical load ratings are typically bending, shear, or axial stresses. The corresponding capacity of the rated member is based on the material and sectional properties as well as the rating level. Based on the deck type and beam orientation, the design load distribution factor for analytical rating is calculated based on guidelines provided in AASHTO's *Specifications for Highway Bridges* [2]. Initial calculations determine the required load of the test truck and the positions to load to produce maximum effects on a bridge. For diagnostic load testing, the test truck should be heavy enough to represent anticipated service loads while not placing any portion of the bridge under nonlinear behaviour [1].

AASHTO standard trucks — including the HS20-44 — are hypothetical trucks developed for standardizing the design and load rating of bridges. Pursuant to local state regulations, bridges are typically load rated for several different truck types so trucks with different axle configurations are included. During this project, four additional hypothetical trucks used by the Kentucky Transportation Cabinet (KYTC) were included in the rating analysis. The load posting, if required, would be based on the lowest of these ratings. Truck axle positions and loading are detailed in Table 1. The posting load is calculated by multiplying the RF by the weight of the posting truck.

While load rating is done using standard truck types, when load testing any suitable truck loaded to a predetermined weight can be used.

Table 1 Load Rating Truck Details

AASHTO & Kentucky load rating trucks		
Truck Type	**Axle location and weight distribution**	**Truck Weight (Tons)**
HS20		36.00
KY TYPE 1		20.00
KY TYPE 2		28.35
KY TYPE 3		36.75
KY TYPE 4		40.00

Eq. 1 is used to evaluate the load rating based on field load test results. Dead and live load effects, when utilizing load test data, are typically strain or corresponding stress values. The load rating through field load test results can be determined based on guidelines in NCHRP's *Manual for Bridge Rating through Load Testing* [8], which is summarized in Chapter 8 of the MBE [1]. The

manual provides an adjustment factor (K), based on field test results and other criteria, to modify the RF previously calculated (Eq. 1). Eq. 2 is the modification to the rating equation.

$$RF_T = RF \times K \qquad\qquad (2)$$

Where:

RF_T = Load rating factor based on field test

RF = Rating factor from Eq. 1

K = Adjustment factor

The adjustment factor, K, is calculated using Eq. 3:

$$K = 1 + K_a \times K_b \qquad\qquad (3)$$

K_a accounts for both the benefit derived from the load test, if any, and consideration of the section factor resisting the applied test load. It is given by the general expression below:

$$K_a = \frac{\varepsilon_C}{\epsilon_T} - 1 \qquad\qquad (4)$$

Where:

ε_T = Maximum member strain measured during load test

ε_C = Corresponding theoretical strain due to the test vehicle and its position on the bridge

K_b accounts for the understanding of the load test results when compared to those predicted by theory, the type and frequency of follow-up inspections, and the presence or absence of special features such as non-redundant framing and fatigue-prone details. The K_b factor is as follows:

$$K_b = K_{b1} \times K_{b2} \times K_{b3} \qquad\qquad (5)$$

The three compounded factors are evaluated using the tables provided in NCHRP's *Manual for Bridge Rating through Load Testing* [8]. Note that the MBE [1] does not include K_{b1} and K_{b2} in the calculation of K_b.

K_{b1} takes into account if the behavior of the rated member could be extrapolated, and is linear elastic, at 1.33 times the rating vehicle. The factor also accounts for the ratio between the test vehicle effect and the rating vehicle effect, providing a range of values for K_{b1} between 0 and 1.0. K_{b2} accounts for the type and frequency of bridge inspection; it varies from 0.8 to 1.0. K_{b3} looks at

the presence of critical features that may lead to fatigue- or fracture-induced failure; it varies from 0.7 to 1.0.

The live load effect, L, is significantly influenced by the live load distribution factor. Provided that all the girders have the same section properties and sufficient strain gauges are deployed at the same location on all longitudinal beams, the actual distribution factor for a particular girder can be calculated with the following equation:

$$DF_{T_k} = \frac{\varepsilon_k}{\varepsilon_{total}} \qquad (6)$$

Where:

DF_{T_k} = Test load distribution factor for girder k

$$\varepsilon_{total} = \sum_{i=1}^{n} \varepsilon_i$$

ε_k = Strain measured in girder k for a given load case

ε_i = Strain measured in girder i for a given load case

n = Total number of girders

The initial analytical load RF from Eq. 1 can be revised based on the actual live load distribution factor, replacing the live load distribution factor taken from AASHTO's *Specifications for Highway Bridges* [2]. Provided the distribution factor calculated with Eq. 6 using the strains observed during the field test is less than what is obtained from the AASHTO Specifications [2], an immediate increase in load rating will be seen. The revised RF should be used to evaluate the rating factor based on the field test by modifying Eq. 2 with the adjustment factor K.

3. Magnetic Strain Gauges

Sensormate's QE-1010 magnetic strain gauges were the first strain gauges evaluated. These gauges adhere to the steel surface through magnetic forces rather than the traditional adhesives used for foil-type strain gauges. The friction between the surfaces is intended to replace the bonding. Strain gauges were coupled with SG-Link-MXRS type sensor nodes and a MicroStrain Inc. base station to create a wireless data acquisition system. The greatest advantage of these gauges is the reduced application time compared to traditional foil-type gauges. The wireless capabilities of the data acquisition system also reduce the time and effort spent on connections, and sometimes diagnosis. Because they are not adhesively bonded, the gauges are reusable. The steel surface must be ground and cleaned with a solvent to remove loose debris and establish a smooth and clean bonding surface before the gauges are applied. Laboratory tests were run on a steel plate under pure tension and a W10×22 steel beam in flexure using magnetic strain gauges and traditional bonded foil-type strain gauges. For the tension test, four magnetic gauges and two foil-type gauges were applied to the plate (Fig. 1(a)) and tested with a universal testing machine (Fig. 1(b)).
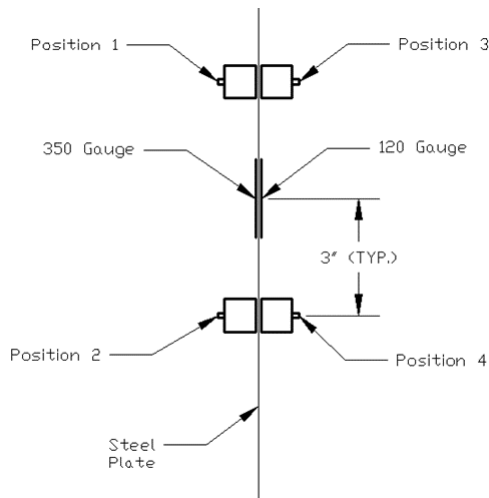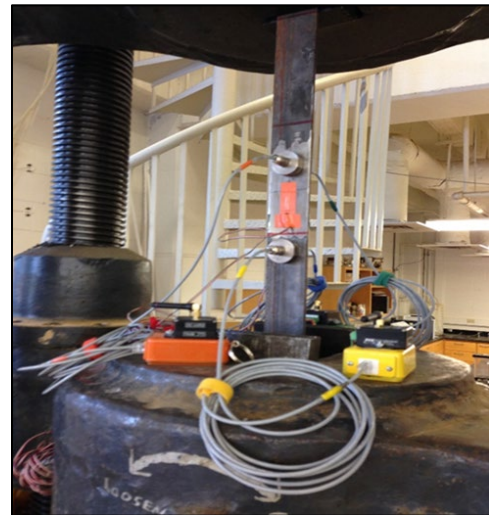

| (a) Gauge layout | (b) Tensile Test |

Fig. 1 Magnetic strain gauge test layout

For each trial, a specimen was loaded multiple times and data were recorded. The effect of surface preparation was evaluated by attaching the magnetic gauges to both cleaned and uncleaned surfaces on the steel plate. The result of one of the trials, where only three magnetic gauges were used, can be seen in the plot in Fig. 2. Strain readings obtained from magnetic gauges were very close to those measured by foil-type gauges. When attached to a mechanically cleaned surface, at higher strains the magnetic gauge slipped, leading to more pronounced differences in readings. However, at low strains, the magnetic gauges exhibited accurate results. When the surface had rust or paint, the slipping and variation from the foil-type gauge readings occurred at lower strains.
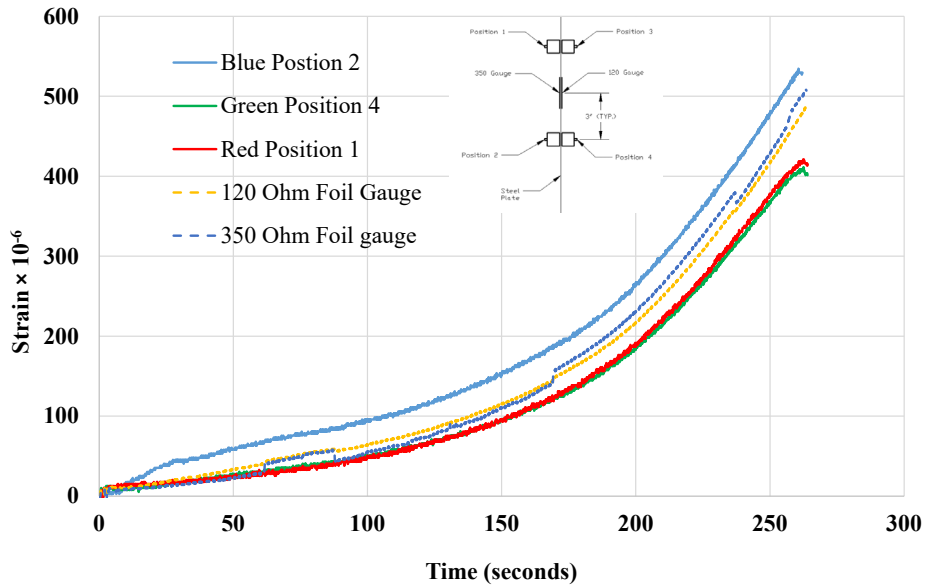
Fig. 2 Tensile test results

Flexural beam tests were conducted on two W10×22, 9-foot simply supported steel beams. Both beams had a C7×9.8 channel section welded to the top to replicate a concrete deck. The beams were part of a separate research project being conducted in the laboratory, and the bottom flange of one beam was strengthened using carbon fiber reinforced polymer (CFRP) laminates while the other was strengthened with CFRP rod panels. Magnetic gauges were attached on one side of the web, while foil-type gauges were mirrored on the opposite side. Fig. 3 shows the layout of the magnetic gauges. Each beam was loaded three times, each test at a different load rate. While at low strains both magnetic and foil-type strain gauges matched well, at higher strains differences were observed. A typical loading is shown in Fig. 4 at location CW3 near the bottom of the web.

Based on the laboratory tests, researchers determined that the magnetic gauges accurately record strains along a bridge beam profile, provided they are attached to a clean surface, the load is applied slowly, and expected strains are less than 400 microstrain. The reusable nature of the gauges, along with the wireless interface, provides an economic advantage when they are used to measure data at remote bridge locations.

Fig. 3 Magnetic gauges mounted on steel beam
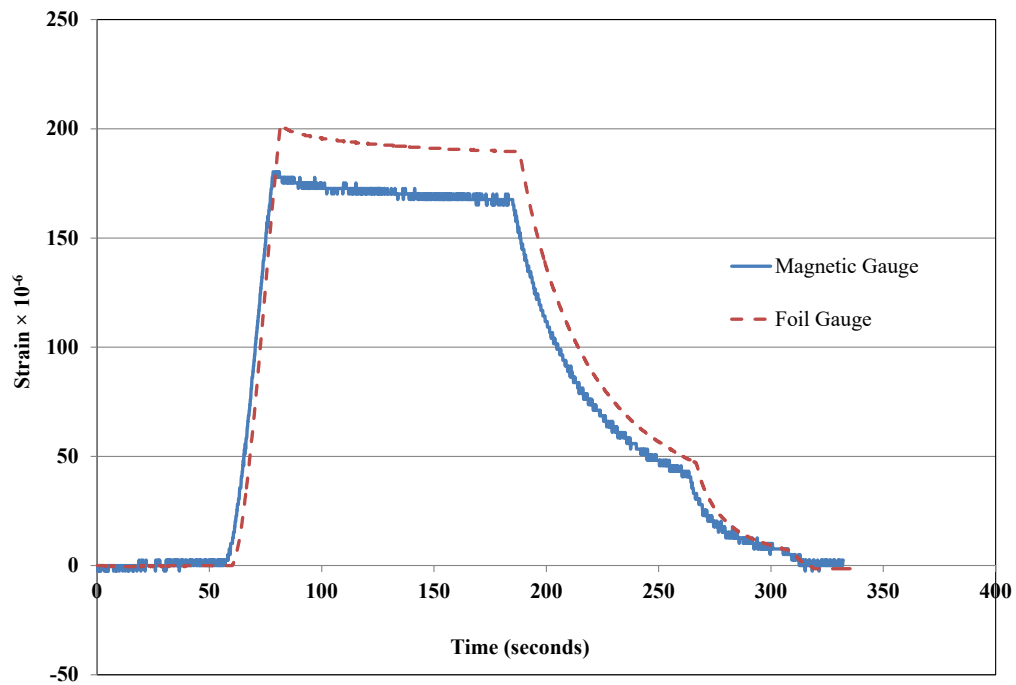
Fig. 4 Beam test results at location CW3

4. Lewis County Bridge Testing

To fully test the functionality of the magnetic gauges, a field test was performed on the KY 1068 Bridge over Laurel Creek in Lewis County, Kentucky (068B00057) (Fig. 5). The bridge is 61'6" long and 26'2" wide. Its original construction date is unknown. In 1954 the structure was expanded from a single lane to a double lane bridge by adding two additional girders on one side. The present construction of the bridge includes four W33×130 girders with a 6.5" non-composite concrete deck. The two original steel beams were constructed by splicing three smaller beams together, with diagonal cross bracing between the spliced beams. The two new beams have no splicing and transverse floor beams as bracing at third points. All the steel beams are spaced 6'0" apart. The concrete deck was cast to cover the steel beam top flanges, while the beam ends were embedded in the deck over the abutment.

Fig. 5 KY 1068 Bridge over Laurel Creek

4.1. Load Rating: AASHTO

The study aimed to evaluate the maximum load carrying capacity under different truck types. An LFR, based on the bridge plans and estimated material properties, was carried out according to AASHTO's MBE [1] and compared with the load rating obtained through field load testing. The load rating through field load testing was calculated based on the procedure discussed in Chapter 2. Prior to testing the bridge was load posted at 17 tons.

Material properties were estimated based on the construction period. The steel's yield strength was assumed to be 33 ksi, while the concrete was assumed to have a compressive strength of 3,500 psi. Five load rated trucks (HS20 and KY Type 1 – 4) with different axle distributions were placed on the girder to provide maximum stresses at mid-span under simple support conditions. The live load moment distribution and impact factor were calculated according to guidelines. Since the bridge

was constructed to be non-composite without shear connectors between the steel beams and concrete deck, the steel beam's moment capacity was calculated based on the section properties obtained for a W33×130 section from the AISC *Steel Construction Manual* [9]. Deflections, overloads, and other serviceability criteria were not considered. The AASHTO LFR was calculated using Eq. 1 (see Chapter 2). A calculated load distribution factor of 1.09 per wheel lane and an impact load of 27% of live load were included in the rating. Appendix B contains details of the load rating calculation for the HS20 truck.

4.2 Field Load Testing

Field load test was carried out using a loaded dump truck weighing 30.85 tons. The individual weights of each axle of the test truck and the axle distribution are shown in Fig. 6. Due to the girder location, the two interior girders would carry most of the live load. The axle position producing the greatest live load moments was expected to be where the rear axles of the test truck were placed at mid-span. Since the bridge section at mid-span is nonsymmetrical due to the two interior beams being constructed in two distinct periods, three transverse axle positions (Fig. 7) were tested to determine which position produces the largest strains in the steel girders. With Load Cases 2 and 3, the rear axles straddled each of the two interior girders; for Load Case 1 the rear axles were positioned with the tire footprints atop both interior girders. Load Case 1 was designed to obtain the maximum load on both center beams and determine if the truck's weight still distributed to the exterior girders. Load Case 2 only tested the interior beam of the new construction, and Load Case 3 only tested the interior beam from the original construction.
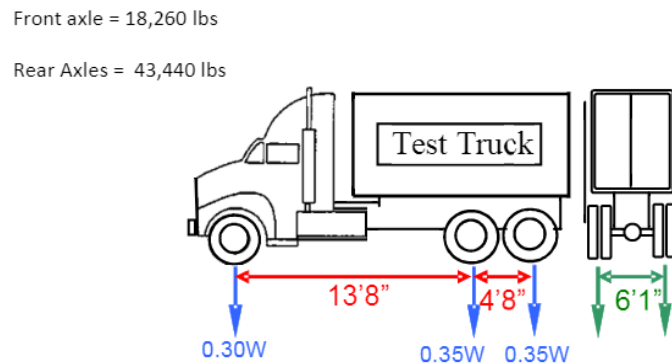
Fig. 6 Field load test truck

For gauge installation, girders were accessed via a trailer-mounted work platform deployed from the top of the bridge. The locations for both magnetic and foil-type strain gauges were cleaned using a mechanical grinder. Nine foil-type strain gauges and four magnetic strain gauges were installed on the steel girders. The magnetic gauges were evaluated against the traditional foil-type strain gauges for possible future deployment in load testing. Strain gauges at the base of the web and bottom flange on all four girders (Fig. 7) were used to evaluate the load distribution. Four foil-type strain gauges and four magnetic strain gauges were placed along the height of the web of one interior beam, while the other interior beam had three foil-type strain gauges. The beam with four gauges (B2) was constructed in 1954, while the other interior beam (B3) with three gauges was an original beam. Gauges were positioned to evaluate the degree of compositeness and estimate the
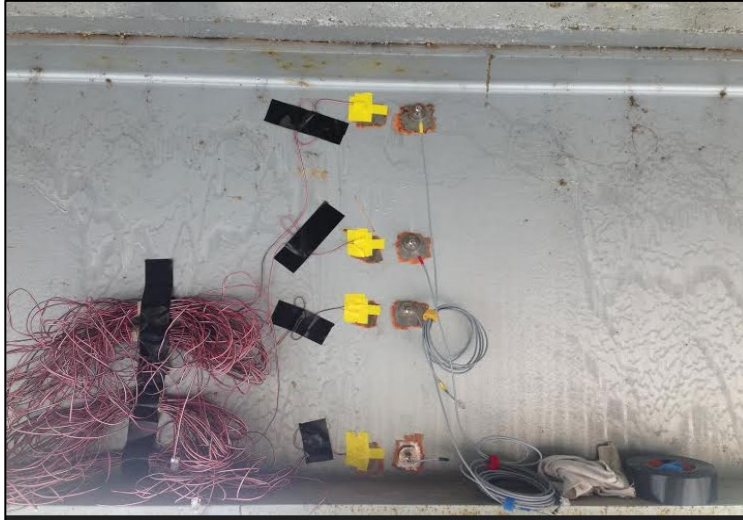
maximum strains on the bottom flange. The gauge set up from the work platform is shown in Fig. 8, while the magnetic and foil gauges mounted on Beam B2 are shown in Fig. 9.
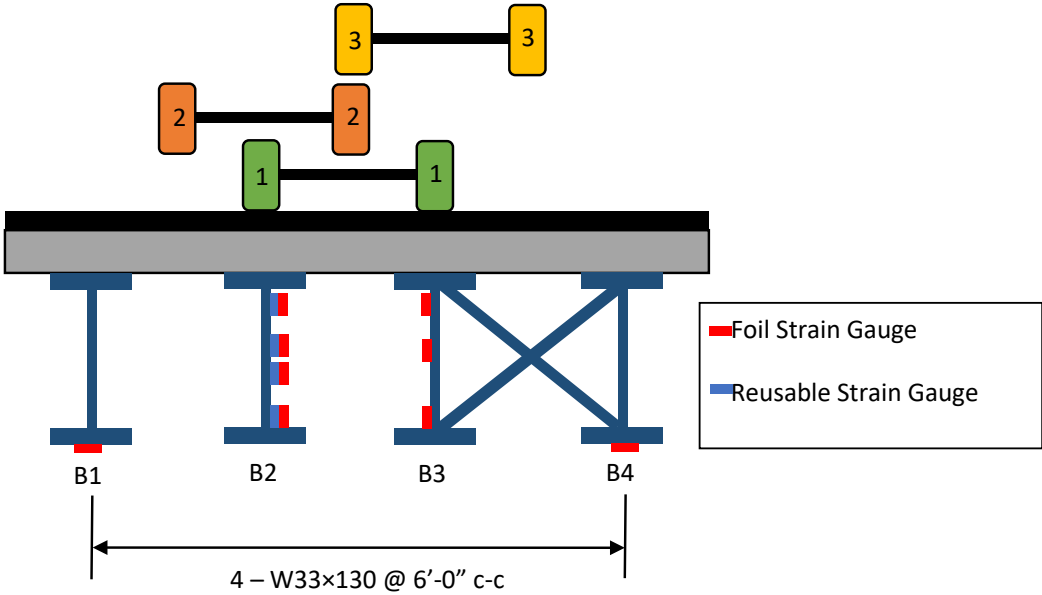
Fig. 7 Field test load cases

Fig. 8 Attaching strain gauges from work platform

Fig. 9 Gauges attached to beam B2

The foil-type gauges were attached to a data acquisition system that was set up near the creek bank using lead wire run along the top of the bottom flanges. Magnetic gauges were attached to the wireless transmitters, with the base station located on the creek bank to receive the signals. While the base station for the magnetic gauges could be powered by a laptop with the batteries within the wireless transmitters already charged, the data acquisition system for the foil-type gauges was powered by a portable generator. Fig. 10 shows the data acquisition set up for both sets of strain gauges. The laptop and base station for the magnetic gauges are on the left; the data acquisition system, laptop, and generator for the foil-type strain gauges are on the right side of the table.

Fig. 10 Data acquisition setup near creek bank

Fig. 11 Load truck axle and tire placement

To evaluate the bridge's longitudinal symmetry under test truck loads, the rear axle was positioned at the three locations (see Fig. 7), with the front axle situated on either side of mid-span (facing north or south), corresponding to six different load positions. Girder lines were marked on the concrete deck above, and the load test truck tires were placed at pre-marked locations (Fig. 11). Test results show that Load Cases 2 and 3 (LC 2 and LC 3) provided similar strain readings, for both north- (LC 2-2, LC 3-2) and south-facing (LC 2-1, LC 3-1) readings, and were greater in magnitude than the readings for Load Case 1 (LC 1-1, LC 1-2).

Strain gauge readings on Beam B2 for LC 2-1 are shown in Fig. 12, along with the theoretical strain profiles of a simply supported girder and a fixed-fixed girder for comparison. The strain readings show that the partial composite action is negligible for the bridge as the neutral axis from the strain readings is very close to the mid-height of the steel girders. Magnetic gauges performed very well compared to the foil-type gauges. The results also show that the bridge's strain profile is closer to that of a fixed end girder than the assumed simply supported configuration. This validates the initial hypothesis that the current load rating system can underestimate the degree of rigidity of bridge supports. The strain profiles for the different load cases are included in Appendix B.

Appendix B also contains transverse strain distribution plots. These plots were used to develop the load distribution factor for individual girders. The distribution factor (*DF*) for each girder was evaluated for each load case based on Eq. 6 (see Chapter 2). For the two interior girders, the strain at the underside of the bottom flange was extrapolated based on the strain reading along the web. The load distribution for LC 3-1 is shown in Fig. 13.
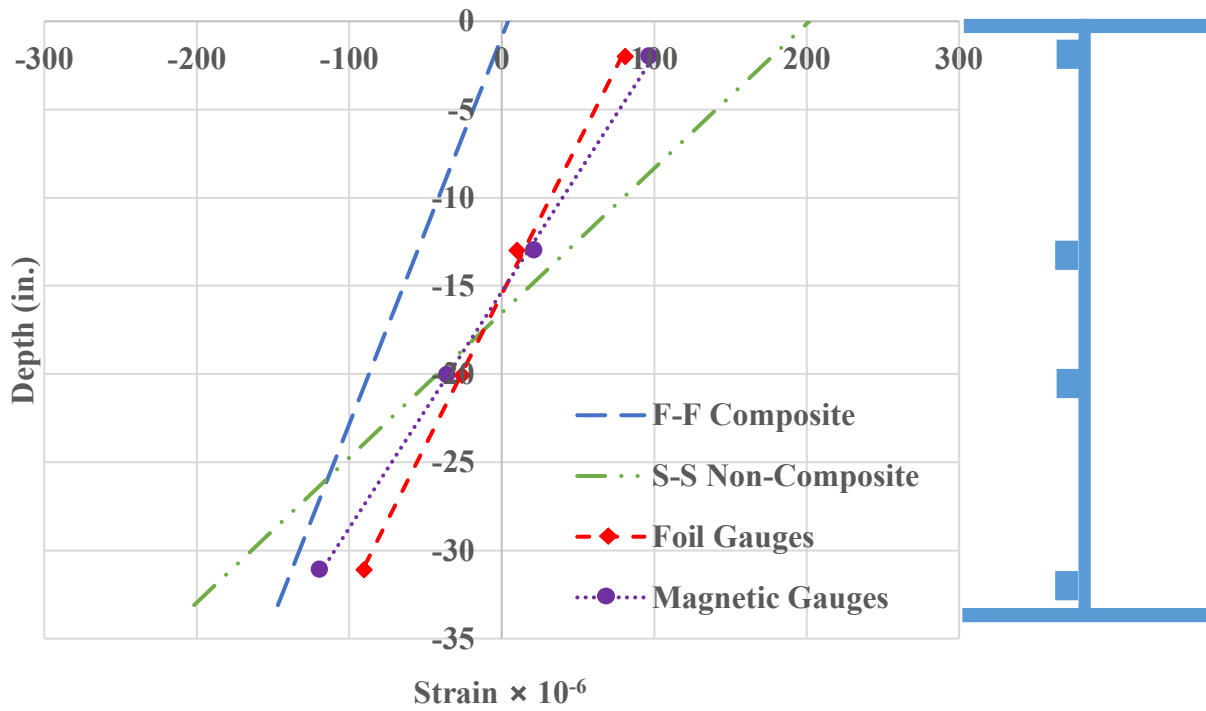
Fig. 12 Field test strain results
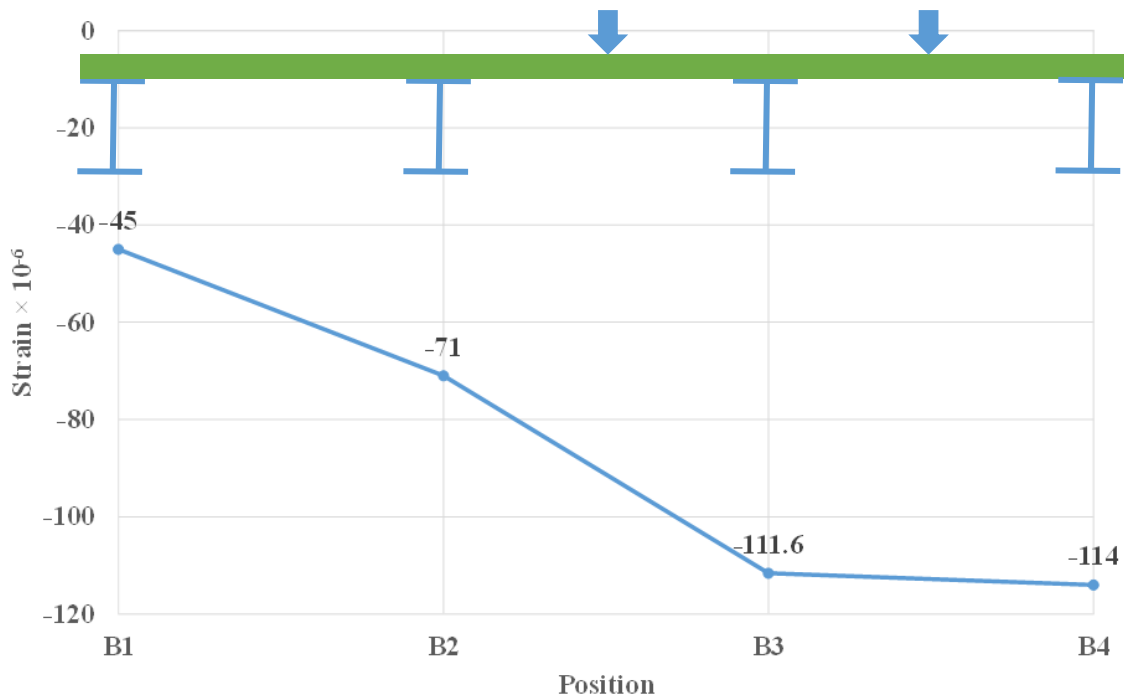
Fig. 13 Transverse strain distribution for LC 3-1

4.3. Load Rating: Field Load Test Data

DFs for the interior beams were calculated by the proportion of strain carried by the girder as described. The *DFs* from the four load positions involving Load Cases 2 and 3 (LC 2-1, LC 2-2, LC 3-1, LC 3-2) ranged from 0.315 to 0.334. The maximum *DF* (0.334) was used to calculate live load moments for the load rating based on field test data.

The maximum strain extrapolated along the bottom flange of the beams from the load tests (ε_T) was 159 microstrains. The K_a factor was calculated by comparing the calculated maximum strain against the theoretical strains at mid-span for the non-composite beam generated by the test truck when using the *DF* evaluated through field load testing.

The factor K_b accounts for an understanding of the test results, type and frequency of follow up inspections, and fracture-critical and fatigue-prone members. The value of K_{b1} depends on the ability to extrapolate the beam member behavior at 1.33 times the load rate truck as well as the ratio between the weights of the load rate truck and the load test truck. Due to the low shear stresses calculated at the steel-concrete interface, and the mostly insignificant composite action between the deck and steel beam, it was estimated the test results could be extrapolated up to 1.33 times the load rate truck. With the test truck live load moment being more than 70% of the live load moment for all the load rate trucks except KY Type 3, K_{b1} was set to 1 for all rating trucks except KY Type 3, for which K_{b1} was 0.8.

K_{b2} depends on the type and frequency of inspections. Based on routine inspections by KYTC every two years, K_{b2} was set at 0.8. In the absence of fracture-critical and fatigue-critical members, K_{b3} was set at 1 for all rating trucks. Appendix B includes the calculation of RF_T for the HS20 truck.

Table 2 summarizes load rating results for Inventory and Operating level ratings for an AASHTO HS20 Truck and Kentucky Legal Truck Types (Type 1-4).

Table 2 AASHTO Load Rating vs. Field Load Testing for Lewis Co. Bridge

AASHTO & KY Trucks		LFR Inventory Rating				LFR Operating Rating			
		AASHTO		Field Load Test		AASHTO		Field Load Test	
Truck	Weight	Rating Factor	Load Posting	Rating Factor	Load Posting	Rating Factor	Load Posting	Rating Factor	Load Posting
	(Tons)		(Tons)		(Tons)		(Tons)		(Tons)
HS20	36	0.594	21	0.92	33	0.991	35	1.54	55
KY Type 1	20	0.877	17	1.37	27	1.464	29	2.28	45
KY Type 2	28.35	0.600	17	0.93	26	1.002	28	1.56	44
KY Type 3	36.75	0.481	17	0.70	25	0.804	29	1.16	42
KY Type 4	40	0.595	23	0.93	37	0.993	39	1.55	61

5. BDI Reusable Strain Gauges

The second type of strain gauge tested in this study was a reusable strain gauge. The gauge selected was the ST350 produced by Bridge Diagnostics, Inc. (BDI), coupled with the STS4 16-channel wireless data acquisition system. Using this set up, all of the strain gauges connect to the STS4 16 channel node, which in turn connects to a STS4 base station that wirelessly broadcasts strain gauge signals to the data acquisition point. It is also possible to connect linear variable displacement transducers (LVDTs) and other types of sensors to the 16-channel node. The ST350 reusable strain gauges have multiple uses and are highly durable due to their rugged, waterproof construction. Compared to magnetic strain gauges, their installation time is high as the tabs they are attached to require adhesive bonding. But, compared to foil-type gauges, the installation is faster and easier. The STS4 system with the 16-channel node and base station for wireless transmission are shown in Fig. 14.
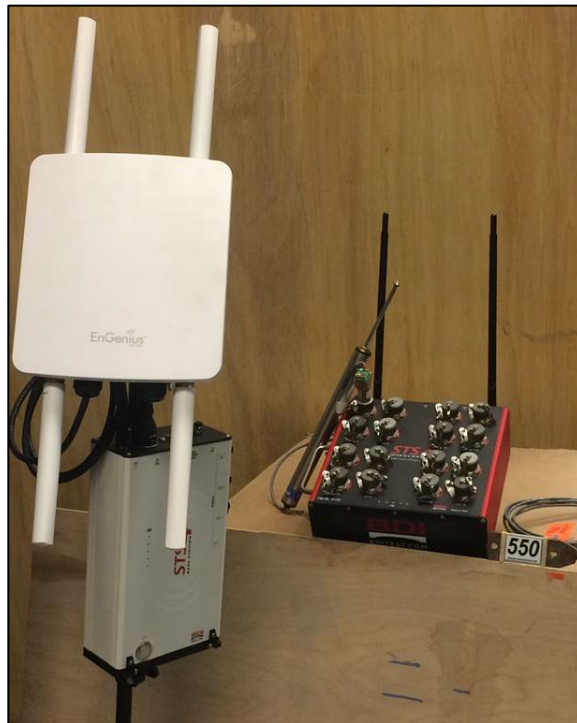
Fig. 14 BDI STS4 system

BDI calibrated the strain gauges, and laboratory tests were conducted to compare the performance of the reusable strain gauges to foil-type strain gauges. Three BDI gauges were attached to the tension side of a beam subjected to 4-point bending. Gauges were attached at the beam's mid-span and quarter-span. At each of these same locations, a foil-type gauge was attached directly below the BDI gauge (Fig.15). The BDI gauges were attached to the 16-channel node and communicated via the base station, while the foil-type gauges were attached to the wired data acquisition system. To evaluate available BDI reusable strain gauges, testing was carried out multiple times, with the three BDI gauges swapped out each time. In addition to the strain gauges, LVDTs were attached

to the STS4 system to measure deflections using the wireless data transmission capabilities. This was in anticipation of possible opportunities where deflections can be measured during bridge field testing. These were evaluated against wire potentiometers connected to the same data acquisition system as the foil-type strain gauges.
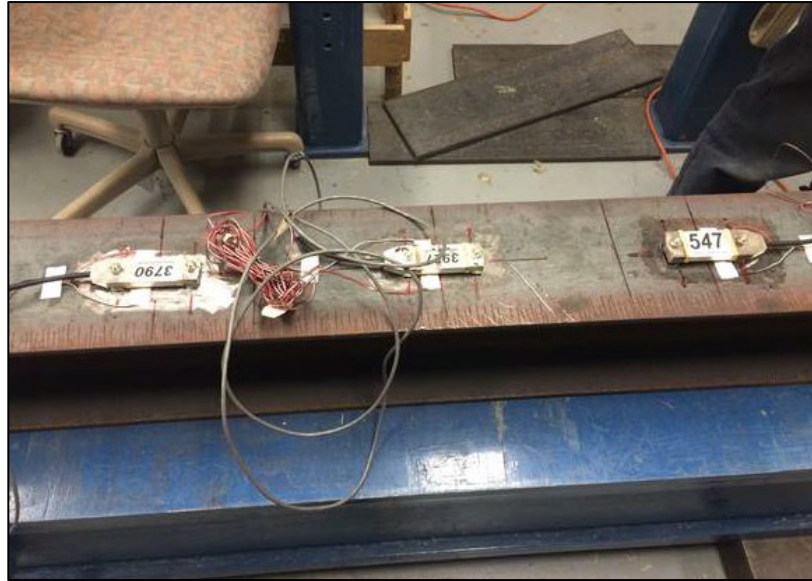
Fig. 15 BDI reusable strain gauges and foil gauges attached to the steel beam

The strain comparison between a BDI reusable strain gauge and a foil-type strain gauge during a stepped load test — where the load was increased and then maintained every 100 microstrain up to a maximum of 500 microstrain — is shown in Fig. 16. Additional test strain comparisons are provided on Appendix E. Laboratory flexural tests showed the BDI gauges matched very well with the foil strain gauges.

Unlike magnetic gauges, laboratory tests found slippage was not an issue for BDI strain gauges. Because the gauges are reusable and rely on a wireless interface, they provide a less expensive option for measuring data at remote bridge locations. One further advantage of the BDI gauges is that multiple gauges can connect to a single transmission base station while retaining the ability to connect to other sensor types (e.g., LVDTs) to measure deflections.
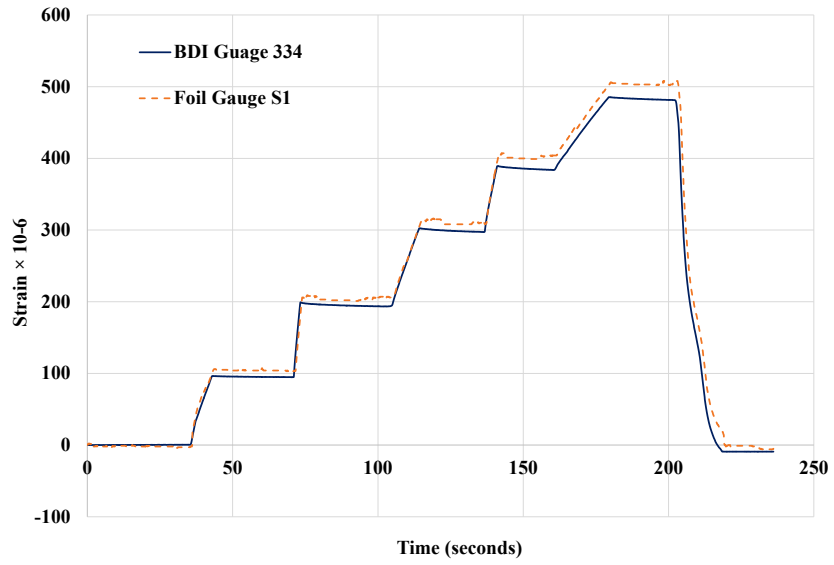
Fig. 16 Strain comparison between BDI reusable gauges and foil gauges

6. Hardin County Bridge Test

As with the magnetic gauges, a field test was conducted to assess the efficacy of BDI gauges. The chosen structure was the KY 220 bridge over Martins Branch Creek in Hardin County, Kentucky (047B00080N). The bridge was built in 1935, and the original design and construction plans were unavailable. The single span bridge is 24'8" long and composed of six W18×50 girders spaced at 4'0" with a 7" non-composite concrete deck on top. The beams are braced by MC9×25.4 channel sections at third points along the main girders. An LFR based on the bridge plans and estimated material properties was carried out following the MBE [1] and compared with the load rating carried out based on field load test results. Before load testing, the bridge had a 17-ton load posting. The profile of the bridge is shown in Fig. 17.

Fig. 17 Hardin County bridge

A large partial composite action between the concrete deck and steel beams was not expected as the concrete deck was not cast atop the steel's flange. There was no visible separation between the bottom of the concrete deck and the top flange of the steel beams. While the steel girders are not encased in concrete at the abutments, the bottom flanges are fixed to the abutment through bolts embedded in the abutment (Fig. 18). Corrosion damage was observed at the ends of nearly all the steel girders. Some of the observed damage is shown in Fig. 18. Since the girder ends and some of the bolt heads were corroded, it is recommended that if the load posting is revised based on the load testing it should be done only after the beam end damage has been addressed.

6.1. Load Rating: AASHTO
An LFR was carried out for an interior beam following the MBE [1]. The material properties were estimated based on the construction period. The yield strength of steel was assumed to be 33 ksi. Five load rated trucks (HS20 and KY Type 1 – 4) with different axle distributions were placed on the girder to provide maximum stresses at mid-span under simple support conditions.

Fig. 18 Bottom flange connection and typical corrosion at beam ends

The live load moment distribution and impact factor were calculated according to guidelines. Since the bridge was constructed to be non-composite, without shear connectors between the steel beams and concrete deck, the moment capacity of the steel beam was calculated based on the section properties for a W18×50 section listed in the AISC *Steel Construction Manual* [9]. Deflections, overloads, and other serviceability criteria were not considered. The AASHTO LFR was calculated using Eq. 1 (see Chapter 2). A calculated load distribution factor of 0.73 per wheel lane and an impact load of 30% of live load were included in the rating. Details of the load rating calculation for the HS20 truck are provided in Appendix F.

6.2. Field Load Testing

The field load test was carried out using a loaded dump truck weighing 20.10 tons. The weights of each axle of the test truck and the axle distribution are shown in Fig. 19. Eight load cases were evaluated to obtain a range of strain and deflection data. Results from the load case that yielded the greatest distribution factor and the maximum moment load case are included in this report. Load Case 1 yielded the largest load distribution factor (Fig. 20). Load Case 2 (Fig. 20) was the maximum moment load case. Due to the bridge's short span, both load cases were controlled by placing the truck's rear axle at mid-span and locating the front axle off the bridge. Two readings were taken for each load case, with the truck facing opposite directions of the bridge.

W = 40,200 lbs

Front Axle = 12,280 lbs

Rear Axle = 27,920 lbs
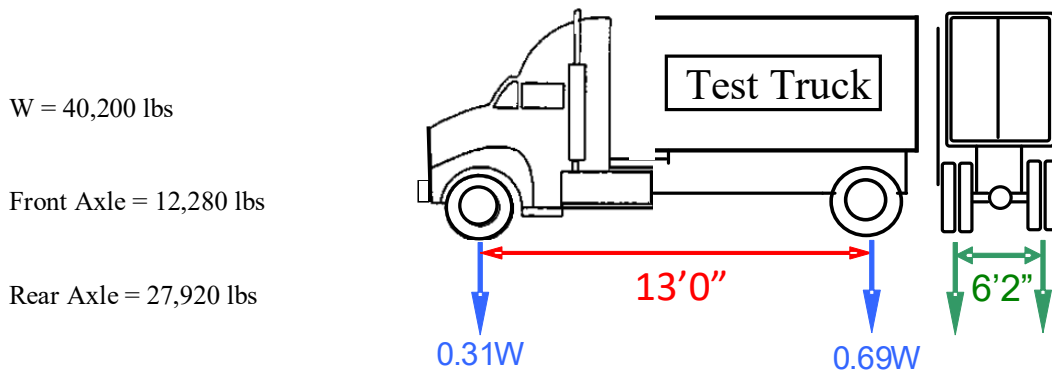
Fig. 19 Field Load Test for the Hardin Co. Bridge
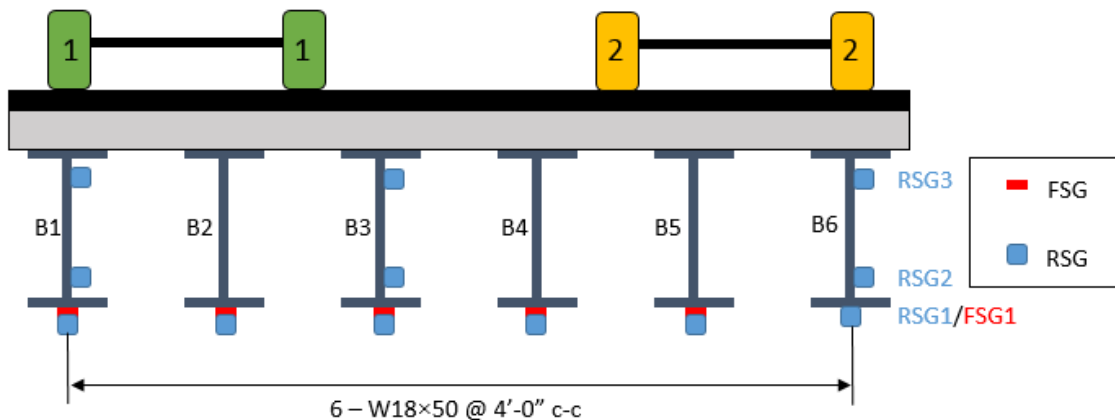
Fig. 20 Load Cases and Gauge Layout for the Hardin Co. Bridge

Twelve BDI reusable strain gauges (RSG) and five foil-type strain gauges (FSG) were placed on the steel girders (Fig. 22). The creek bed was relatively dry during of gauge installation and load testing. Therefore, beams were accessed using adjustable step ladders. BDI reusable gauges were

---

evaluated against foil-type strain gauges for possible future deployment in load testing. Reusable strain gauges on the underside of the bottom flange of all six girders were used to evaluate the load distribution. Foil-type gauges were placed on the underside of the bottom flange of all girders except Girder B6. Two BDI reusable strain gauges were placed along the height of the web of one interior girder (B3) and both exterior girders (B1 and B6). These gauges were placed to evaluate the degree of compositeness. The BDI gauges and the foil-type gauge on the bottom flange of the interior beam are shown in Fig. 21.

Fig. 19 Strain gauges on interior beam

Fig. 20 Layout of data acquisition systems underneath the bridge

In addition to strain gauges, three LVDTs were used to measure the deflection at mid-span of one of the interior girders and one exterior girder as well as at quarter-span of the exterior girder. Because the creek bed was dry, LVDTs were placed on the creek bed against weights hung from the respective locations on the steel beams. Fig. 22 illustrates the LVDTs, data acquisition systems, and their layout underneath the bridge. The BDI STS4 16-channel node was placed on the creek bed, and the BDI reusable strain gauges were attached to the node. The base station with wireless transmitter was placed near an abutment, but the laptop receiving the signal was placed under the bridge. While data acquisition with the BDI gauges was possible without the wireless transmission due to the ease with which the bridge's underside could be accessed, the wireless base station was chosen with future uses in mind. Lead wires from the foil-type strain gauges were attached to a data acquisition system, which in turn was controlled by a laptop. A portable generator powered the system.

As noted, due to bridge's short span, only the rear axle was used in load application. Wheel lines were marked on the concrete deck, and the load test truck tires were placed at pre-marked locations (Fig. 23). Three of the eight load cases were rolling load cases; the remaining five were stationary. One of the five stationary load cases involved placing the rear axle at quarter-span to evaluate the structure's longitudinal loading symmetry. As noted, the results from the load case that yielded the greatest distribution factor and the load case that yielded the maximum moment are included in this report as they provided information to calculate the structure's load rating. The two readings taken for each load case, with the truck facing opposite directions, are designated LC 1-1, LC 1-2, LC 2-1 and LC 2-2.

Fig. 21 Positioning of load test truck on bridge deck

The transverse strain distribution for the two load cases identified in Fig. 20, are shown in Fig. 24. Measured strain from the BDI reusable strain gauges (RSG) and the foil-type strain gauges on the bottom flange of each girder are shown. The highest *DF* of 0.315 was calculated from Load Case 1 (Fig. 24(a)). The largest strain under the test truck was 98.95 microstrain (Load Case 2) (Fig.

24(b)). The strain profile along the depth of a steel girder indicates the degree of compositeness between the steel girder and concrete deck. The profile at Beam 6 (B6) for the maximum moment load case (Load Case 2) is shown in Fig. 25.
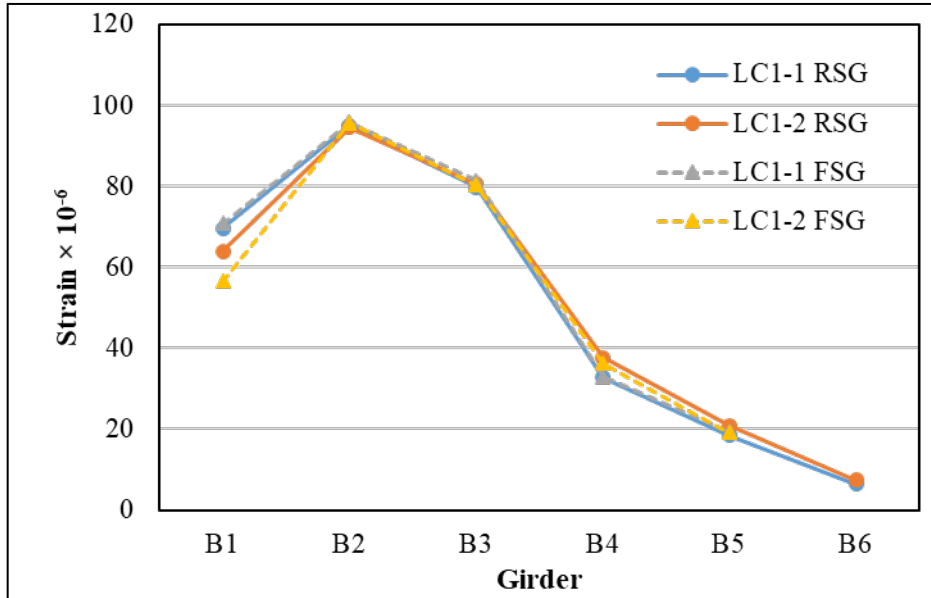
(a) Transverse strain distribution at mid-span for Load Case 1
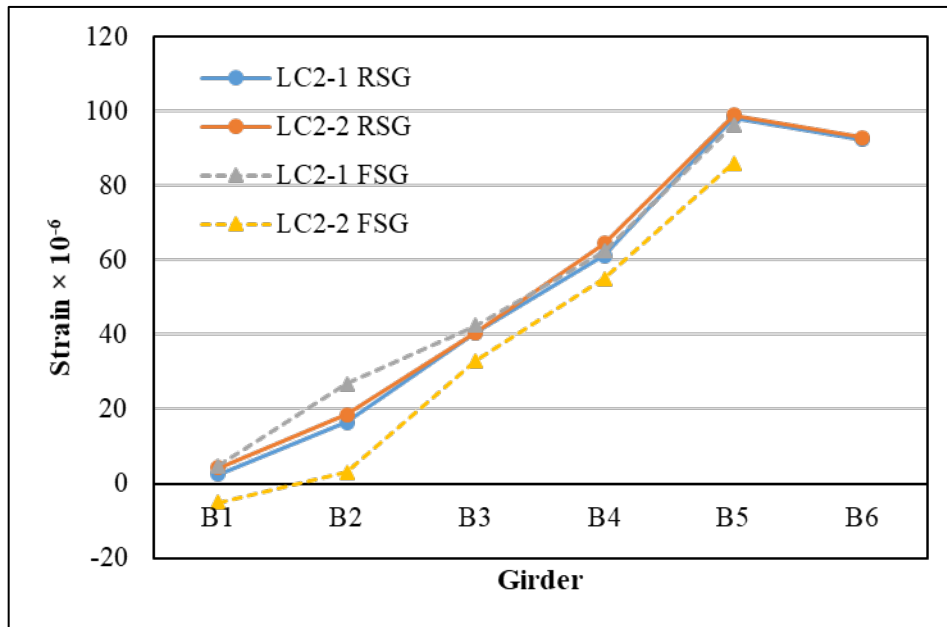
(b) Transverse strain distribution at mid-span for Load Case 2

Fig. 22 Transverse strain distribution
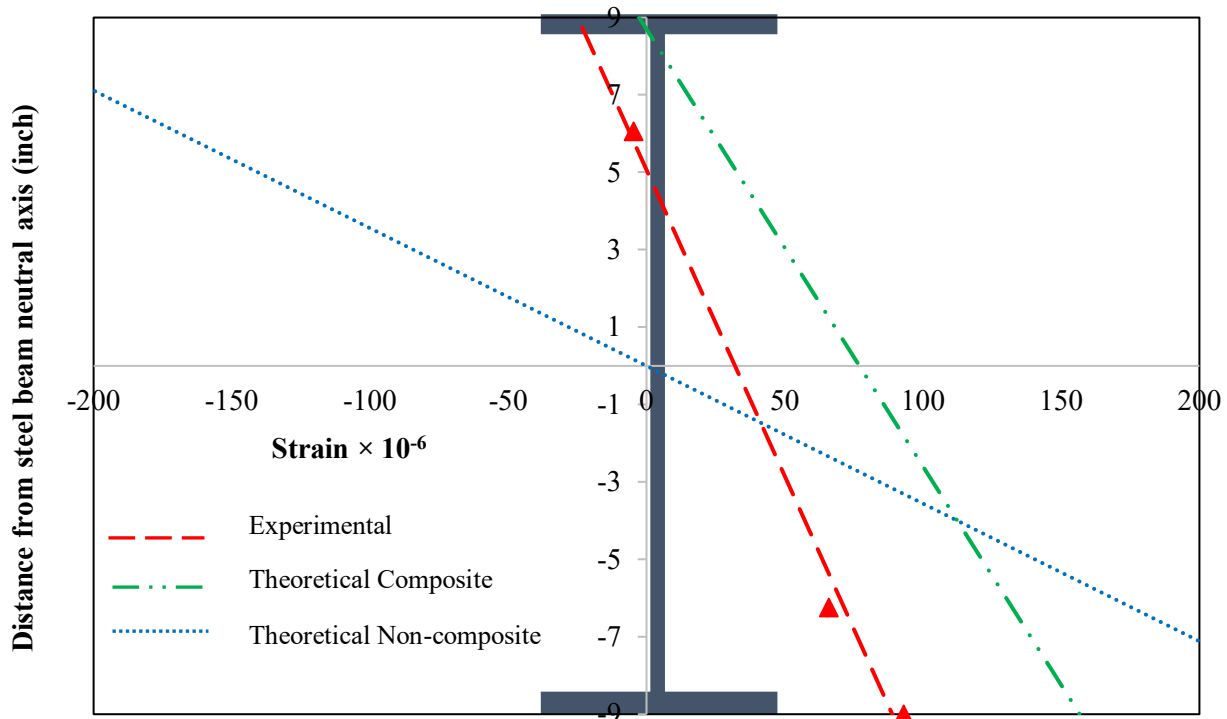
Fig. 23 Strain profile at mid span for Beam 6 (B6) under maximum moment load case (LC 2)

Strain readings recorded along the depth of the interior beams for all load cases showed that the concrete deck and steel girders have a certain degree of compositeness. The strain profile for B6 under Load Case 2-2 (Fig. 25) indicates that the neutral axis lies between the theoretical non-composite neutral axis (at mid-height of the girder) and the theoretical fully-composite neutral axis. The theoretical fully-composite neutral axis was located 0.3 in. below the concrete deck and was calculated from section transformation. Concrete strength was assumed to be 2,500 psi.

6.3. Load Rating: Load Test Data
The *DF* for the interior beam was calculated by the proportion of strain carried by the girder. The *DF* from the five stationary load cases ranged from 0.271 to 0.315. The maximum *DF* (0.315) was used to calculate live load moments for the load rating.

The maximum strain measured along the bottom flange of the beams from the load tests (ε_T) was 98.95 microstrain. This figure was compared to the theoretical strain at mid-span for the non-composite beam generated by the load test truck when utilizing the distribution factor evaluated through field load testing. The factor, K_a, accounting for any benefit observed from the load test was evaluated based on the ratio of the two strains (see Chapter 2).

The factor, K_b, was calculated for each load rating truck type based on the K_{b1}, K_{b2} and K_{b3} values. The value of K_{b1} depends on the ability to extrapolate the beam member behavior at 1.33 times the load rate truck as well as the ratio between the effects of the load rate truck and the load test truck. Due to the peak strains being well below yielding, it was estimated that the test results could be extrapolated up to 1.33 times the load rate truck. With the test truck live load moment being less than 70% of the live load (+ impact) moment of all the load rate trucks except KY Type 4, K_{b1} was set to 0.8 for all rating trucks except KY Type 4, for which K_{b1} was 1.0. K_{b2} depends on the type and frequency of inspections. Assuming routine inspections every two years, K_{b2} was set to 0.8. K_{b3} accounts for critical structural features. In the absence of fracture-critical and fatigue-critical members, K_{b3} was set at 1 for all rating trucks.

The load rating based on the field load test data was carried out for the HS20 truck and provided in Appendix H. Table 3 summarizes the load rating results for Inventory and Operating level ratings for an AASHTO HS20 Truck and Kentucky Legal Truck Types (Type 1-4).

Table 3 AASHTO Load Rating vs. Field Load Testing for Hardin Co. Bridge

AASHTO & KY Trucks		LFR Inventory Rating				LFR Operating Rating			
		AASHTO		Field Load Test		AASHTO		Field Load Test	
Truck	Weight (Tons)	Rating Factor	Load Posting (Tons)	Rating Factor	Load Posting (Tons)	Rating Factor	Load Posting (Tons)	Rating Factor	Load Posting (Tons)
HS20	36	0.916	32	1.83	65	1.529	55	3.05	109
KY Type 1	20	0.916	18	1.83	36	1.529	30	3.05	60
KY Type 2	28.35	0.714	20	1.42	40	1.192	33	2.38	67
KY Type 3	36.75	0.628	23	1.25	46	1.049	38	2.09	76
KY Type 4	40	0.985	39	2.21	88	1.645	65	3.69	147

7. Summary and Conclusions

The current method for load rating bridges — based on AASHTO specifications — can underestimate the capacity and behavior of bridges. Analytical equations do not account for the degree of rigidity in supports, unintended composite action due to friction between girders and the slab, and other factors. Load testing of individual bridges can produce a load rating that much more accurately reflects the capacity of a non-composite bridge. However, current methods of load testing require significant time commitments to instrument a bridge profile to record data, rendering it less feasible. New types of commercially available strain gauges, however, greatly reduce the time required to instrument a location.

This report discussed the load rating of two bridges using field load test data. Researchers evaluated two types of strain gauge in field load tests to determine how effectively they minimize deployment time while maintaining accuracy. Magnetic Sensormate QE-1010 strain gauges and reusable BDI ST350 strain gauges were outfitted with wireless data transmission capabilities for rapid field deployment to determine if using their use would significantly reduce the amount of time required to load test a bridge. For bridges with characteristics such as unintended composite action or end fixity, this would increase the feasibility of load testing bridges, leading to a more favorable load rating. Compared to the theoretical load ratings, ratings based on load tests are expected to be more accurate.

Both gauges were tested in the laboratory under flexural loads. Their readings were compared to those obtained from traditional foil-type strain gauges prior to their deployment on two bridges in Kentucky. Laboratory tests demonstrated the magnetic strain gauges and BDI reusable strain gauges are very accurate at low strains. At higher strains (i.e., more than 400 microstrain) the magnetic strain gauges slipped. The wireless data transmission capability of both systems made it possible to carry out data acquisition without being close to the gauges. This significantly reduced the amount of wiring typically associated with strain gauge data acquisition. While magnetic strain gauges performed well in the field and gauge installation time was reduced, due to the rugged requirements of field testing, they will not be considered for future deployments given the current status of the technology. Reusable BDI strain gauges coupled with wireless transmitters balance rugged performance with short installation times.

Each bridge was load posted because the load rating factor for several truck types was less than one. Table 4 lists the AASHTO load rating and field load testing results for the KY 1068 and KY 220 bridges. Field load tests revealed the load rating factor for strength was adequate for the KY 220 Bridge in Hardin County, while the load rating for the KY 1068 Bridge in Lewis County could be increased by 68%.

Table 4 Load Rating Results

Bridge	Governing Truck Type	AASHTO Analytical Rating Factor	Load Test Rating Factor
KY 1068 – Lewis County	KY Type 3	0.48	0.70
KY 220 – Hardin County	KY Type 3	0.62	1.25

With the development of better, low-cost, wireless, and non-contact sensing technology, field load rating is now a more attainable option for evaluating bridge load ratings. In addition to accurately describing bridge behavior and highlighting unintended factors that may increase load ratings, the technology can also be used to diagnose structural deficiencies.

References

[1]. American Association of State Highway and Transportation Officials. *The Manual for Bridge Evaluation*, Second Edition, AASHTO, Washington, D.C., 2011.

[2]. American Association of State Highway and Transportation Officials. *AASHTO Standard Specifications for Highway Bridges,* 17th Edition, AASHTO, Washington, D.C., 2002.

[3]. Nowak, A.S. and Saraf, V.K., "Load Testing of Bridges", Research Report UMCEE 96-10, University of Michigan, Ann Arbor, MI,1996.

[4]. Schiff, S.D., Piccirilli, J.J., Iser, C.M., and Anderson K.J., "Load Testing for Assessment and Rating of Highway Bridges", Research Project No. 655, Clemson University, Clemson, SC, 2006.

[5]. Jeffrey, A., Breña, S.F., and Civjay, S. "Evaluation of Bridge Performance and Rating through Nondestructive Load Testing", University of Massachusetts Amherst, Amherst, MA, 2009.

[6]. Hosteng, T. and Phares, B. "Demonstration of Load Rating Capabilities through Physical Load Testing: Ida County Bridge Case Study", Part of InTrans Project 12-444, Bridge Engineering Center, Iowa State University, Ames, IA, 2013.

[7]. Hag-Elsafi, O. and Kunin, J. "Load Testing For Bridge Rating: Dean's Mill Over Hannacrois Creek", Report FHWA/NY/SR-06/147, Transportation Research and Development Bureau, Albany, NY, 2006.

[8]. National Cooperative Highway Research Program. *Manual for Bridge Rating Through Load Testing*, NCHRP Project l2-28 (13) A, Transportation Research Board, Washington D.C., 1998.

[9]. AISC Steel Construction Manual (14th Edition).

Appendix A. Magnetic Strain Gauge Test Results
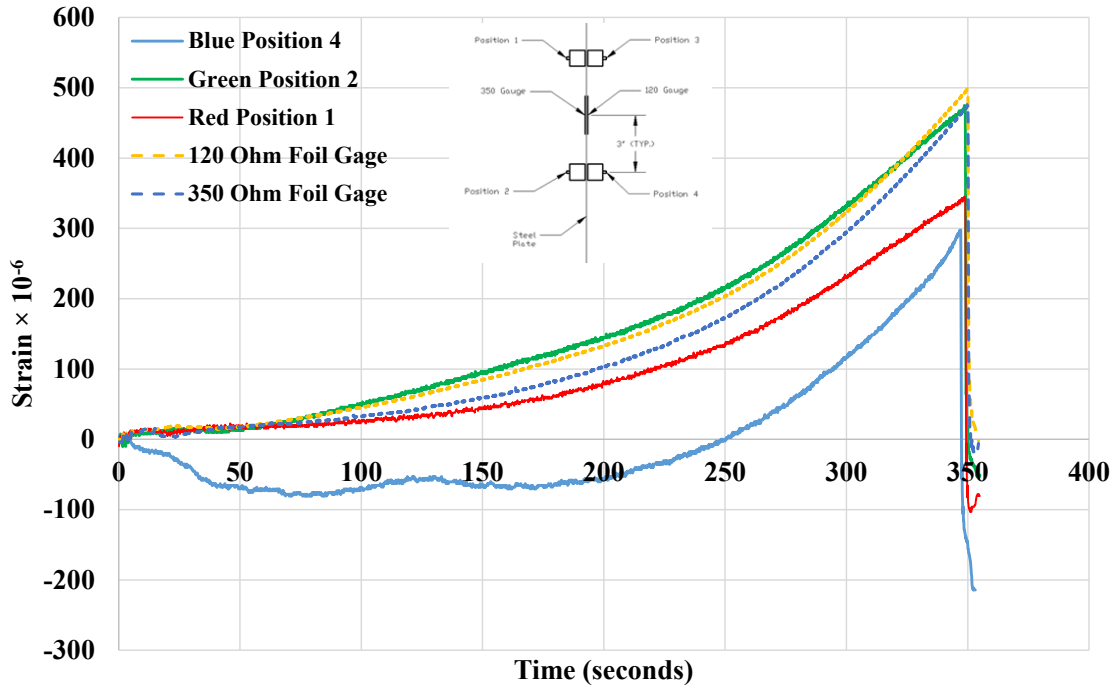
Fig. A1. Tension test 1
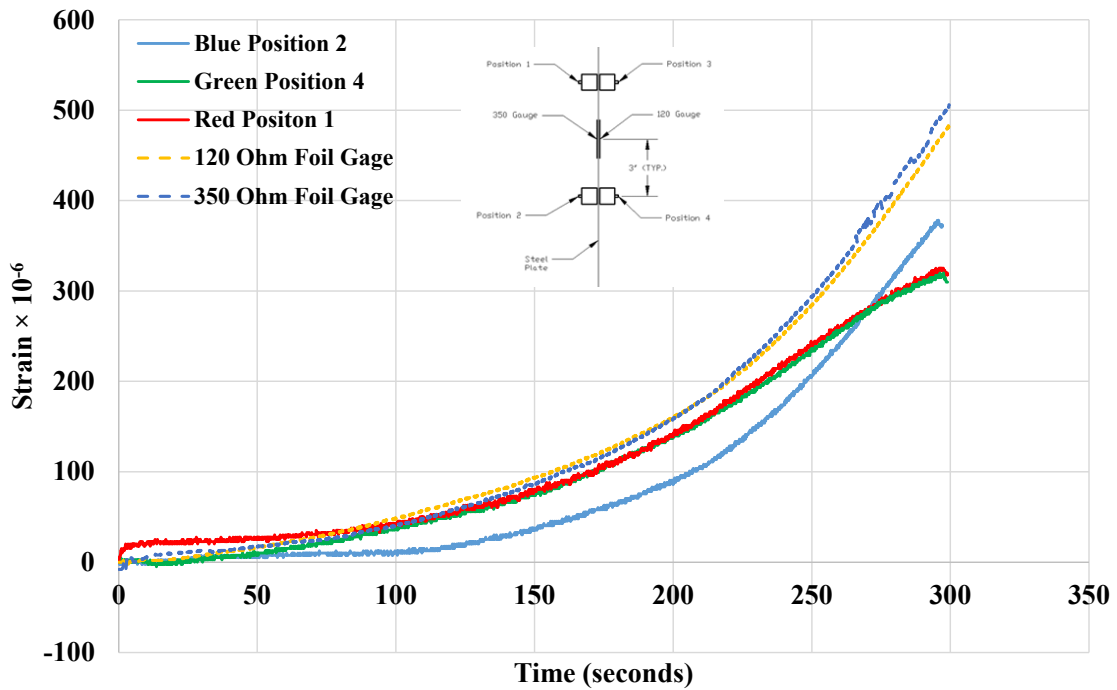
Fig. A2. Tension test 2
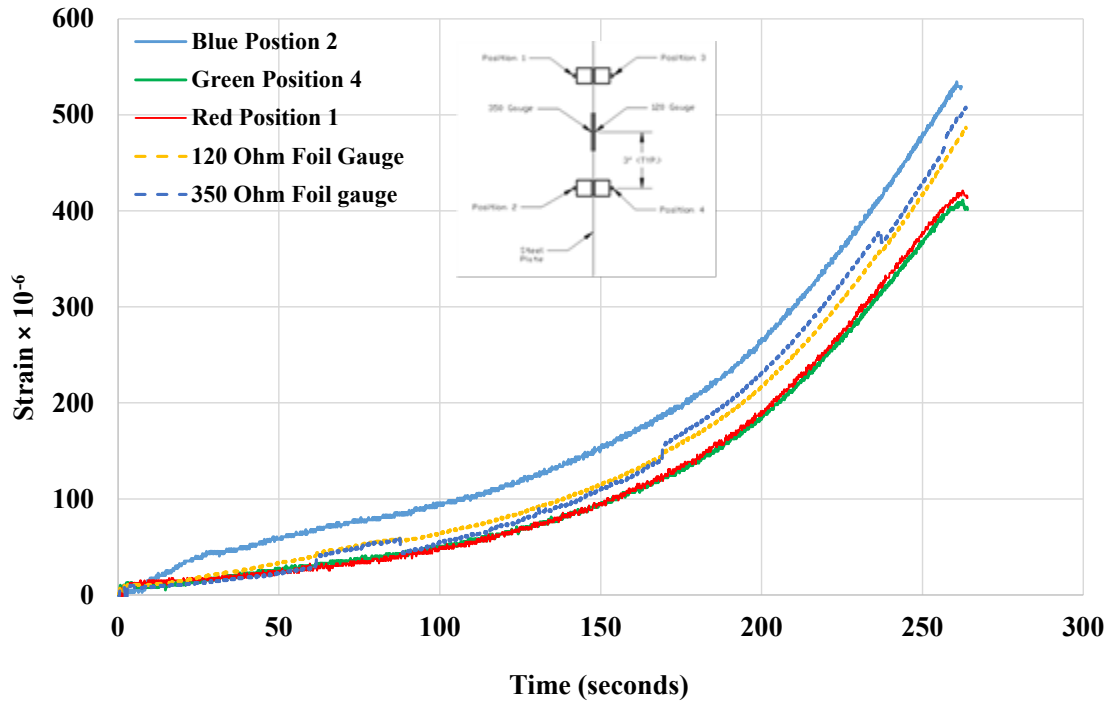
Fig. A3. Tension test 3
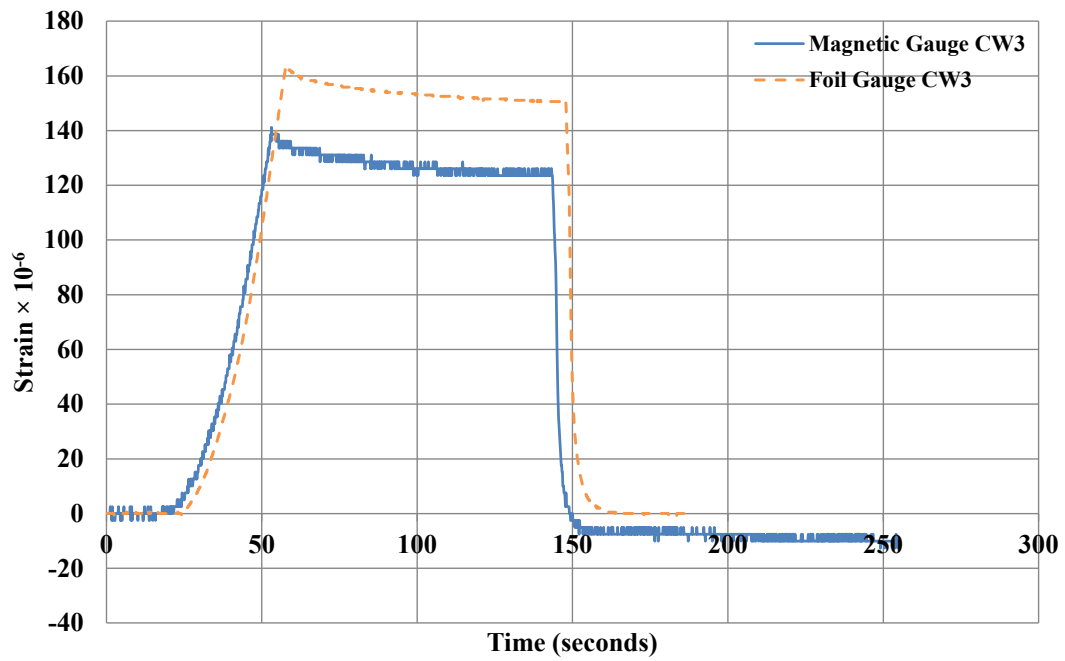
Fig. A4. CFRP splice beam pre load 1 - CW3
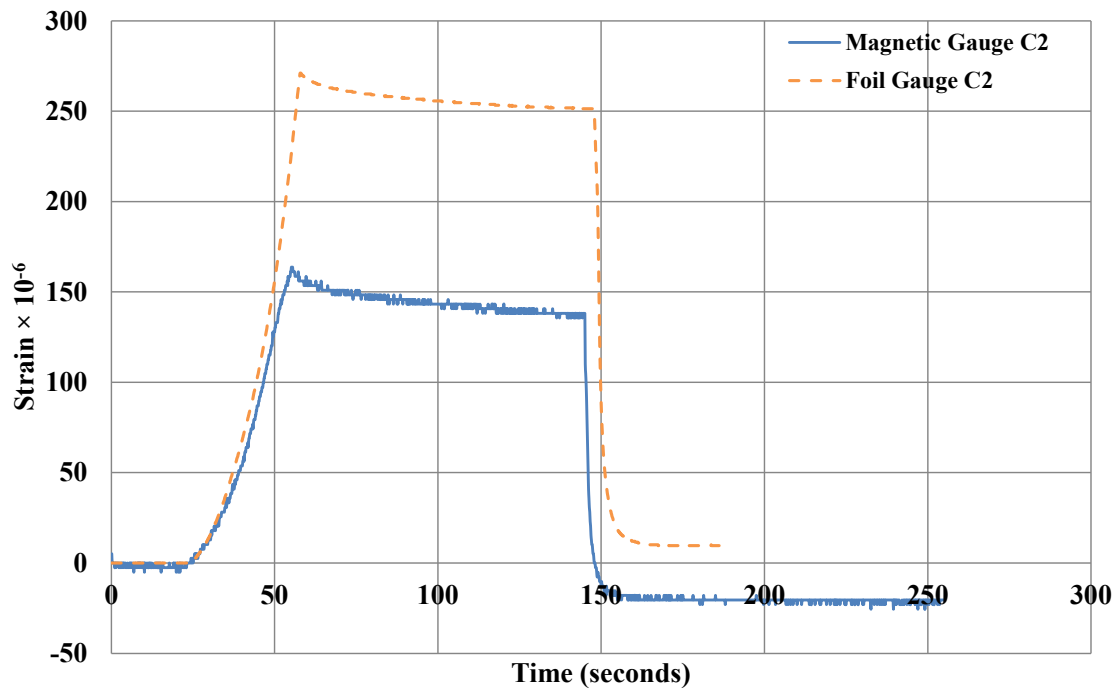
Fig. A5. CFRP splice beam pre load 1 - C2
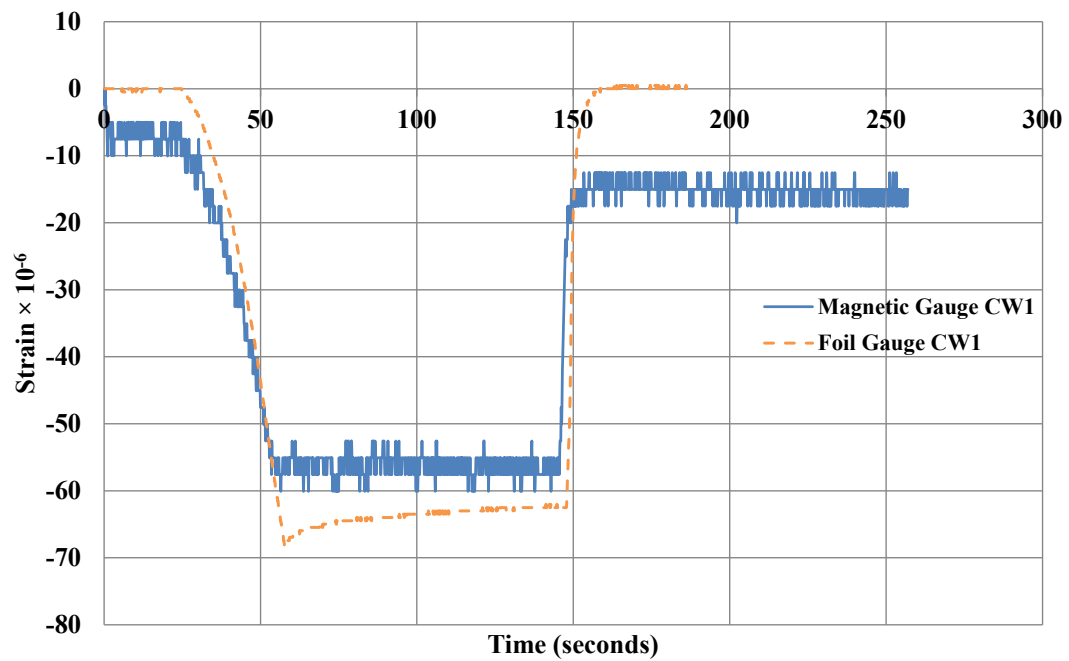
Fig. A6. CFRP splice beam pre load 1 - CW1
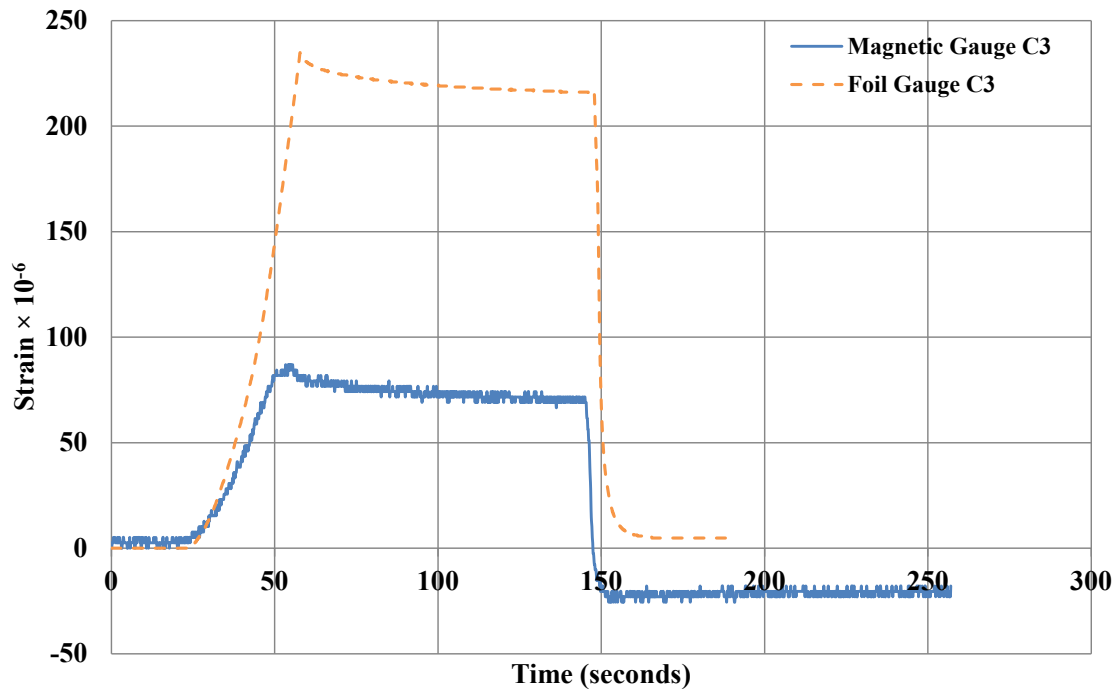
Fig. A7. CFRP splice beam pre load 1 - C3
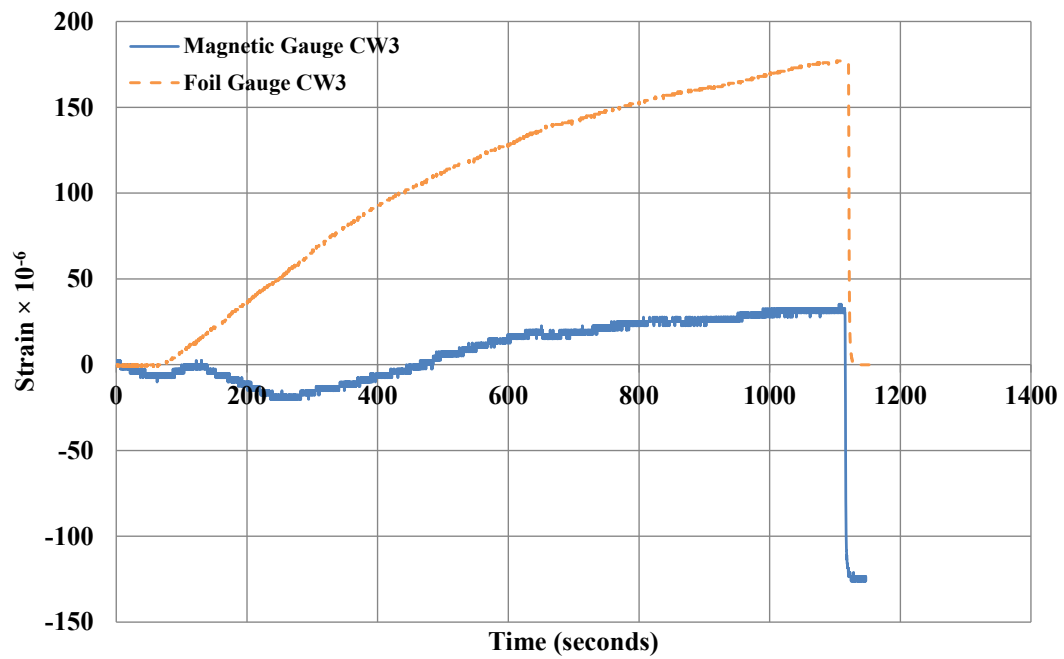
Fig. A8. CFRP splice beam pre load 2 - CW3
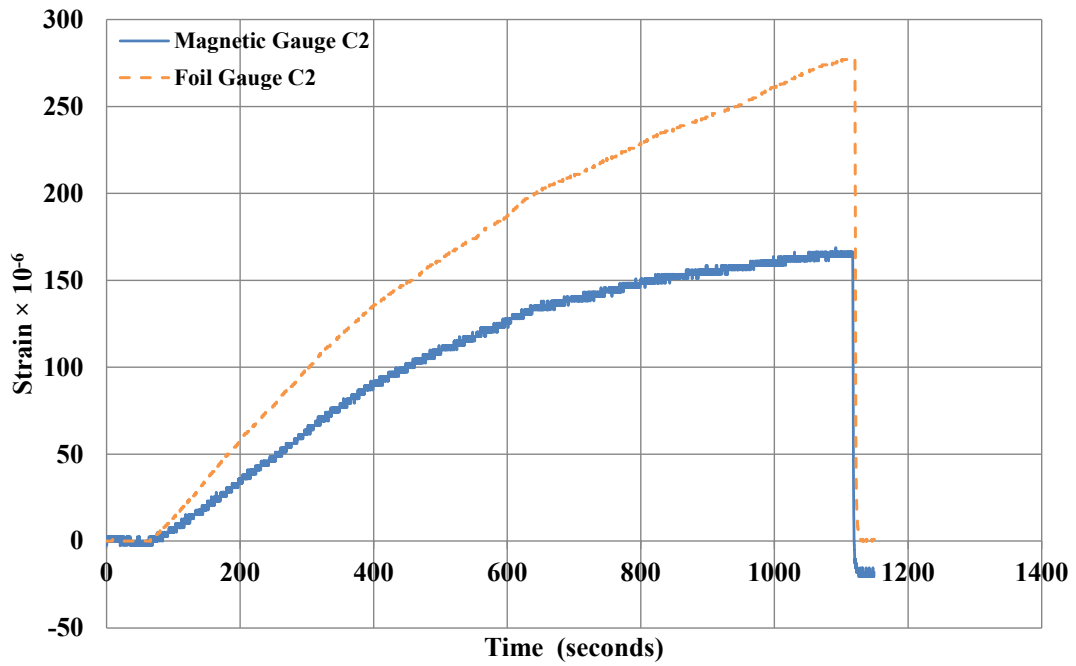
Fig. A9. CFRP splice beam pre load 2 - C2
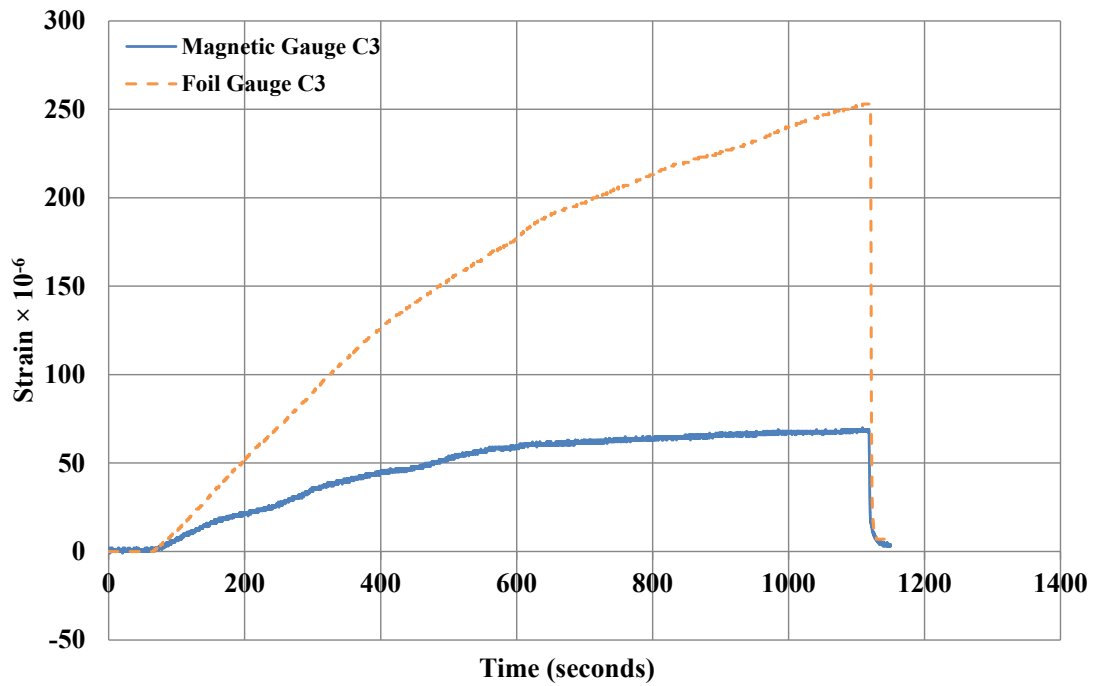
Fig. A10. CFRP splice beam pre load 2 - C3
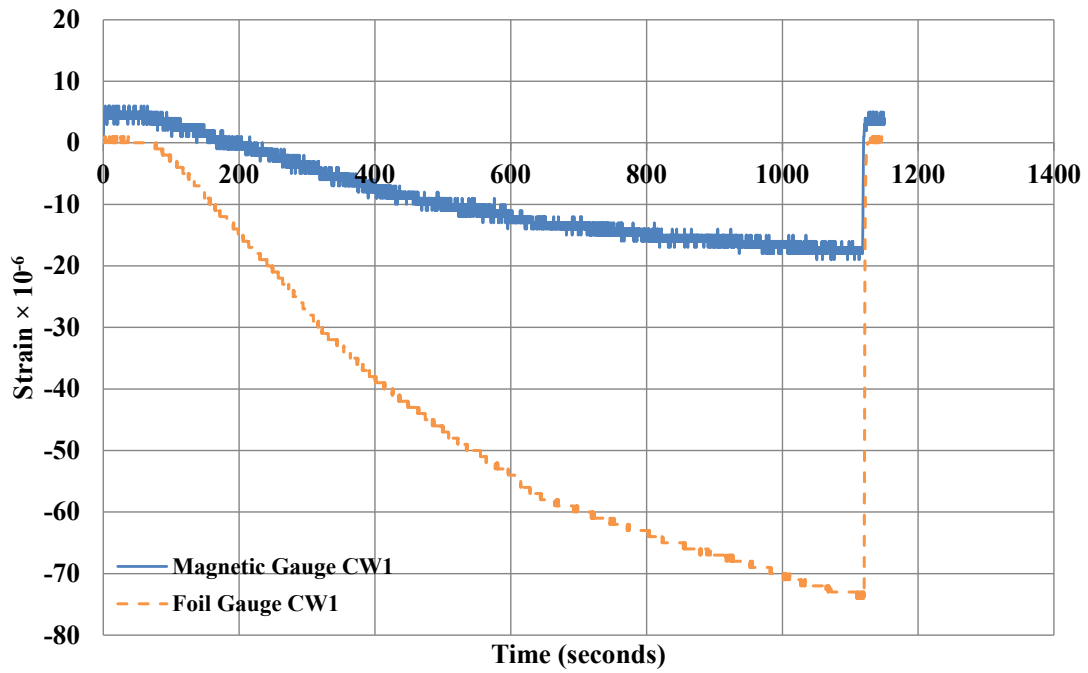
Fig. A11. CFRP splice beam pre load 2 - CW1
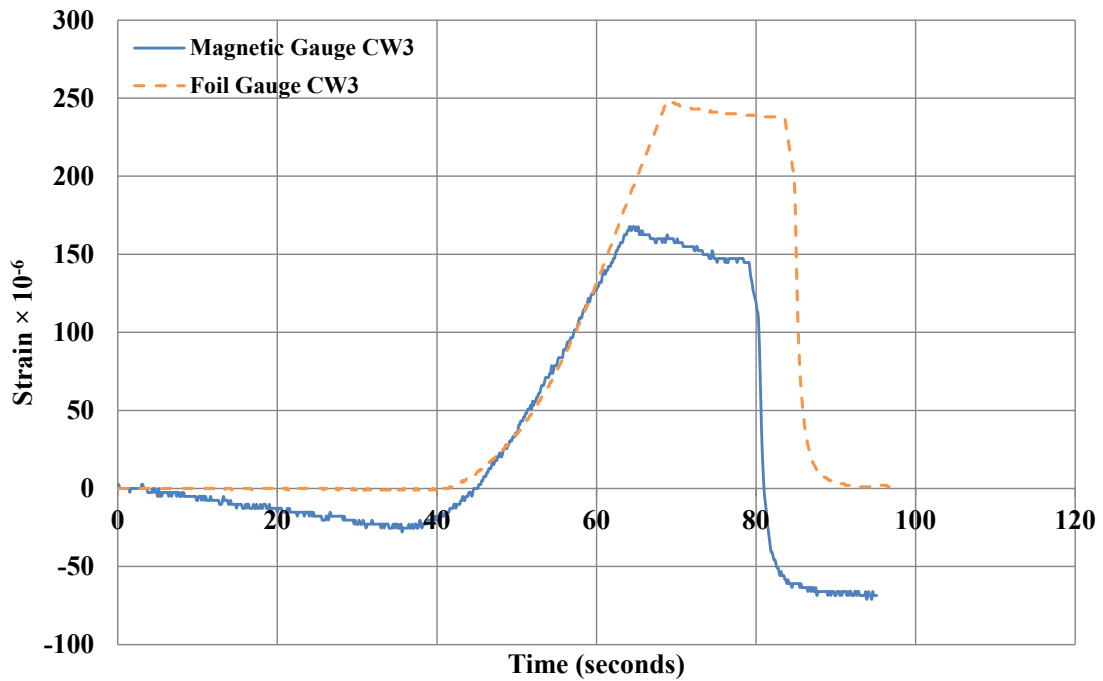
Fig. A12. CFRP splice beam pre load 3 -CW3
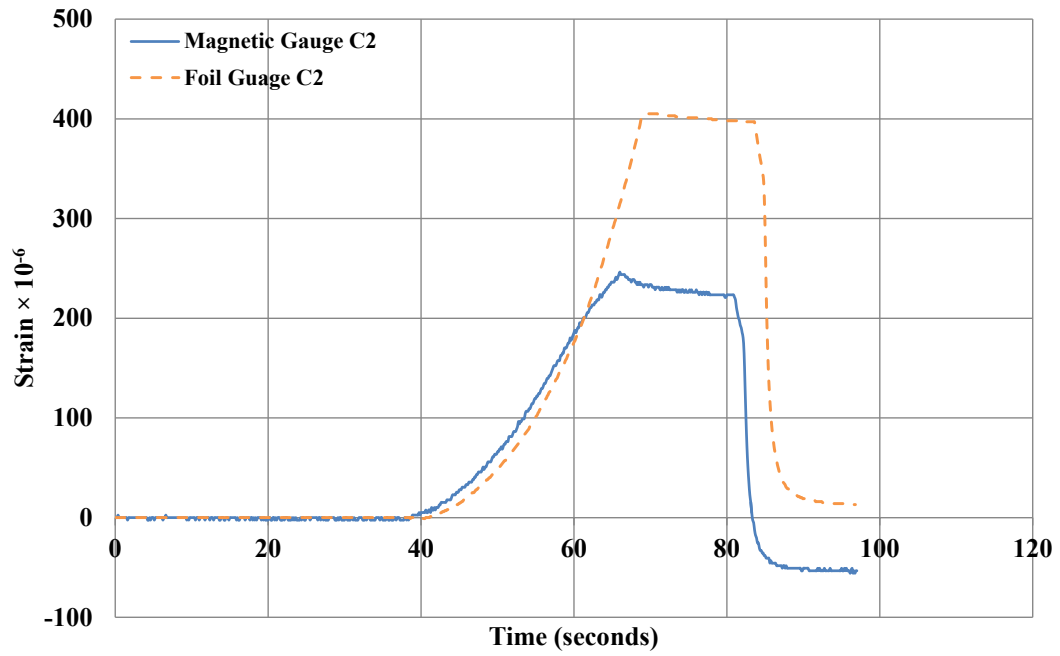
Fig. A13. CFRP splice beam pre load **3 - C2**
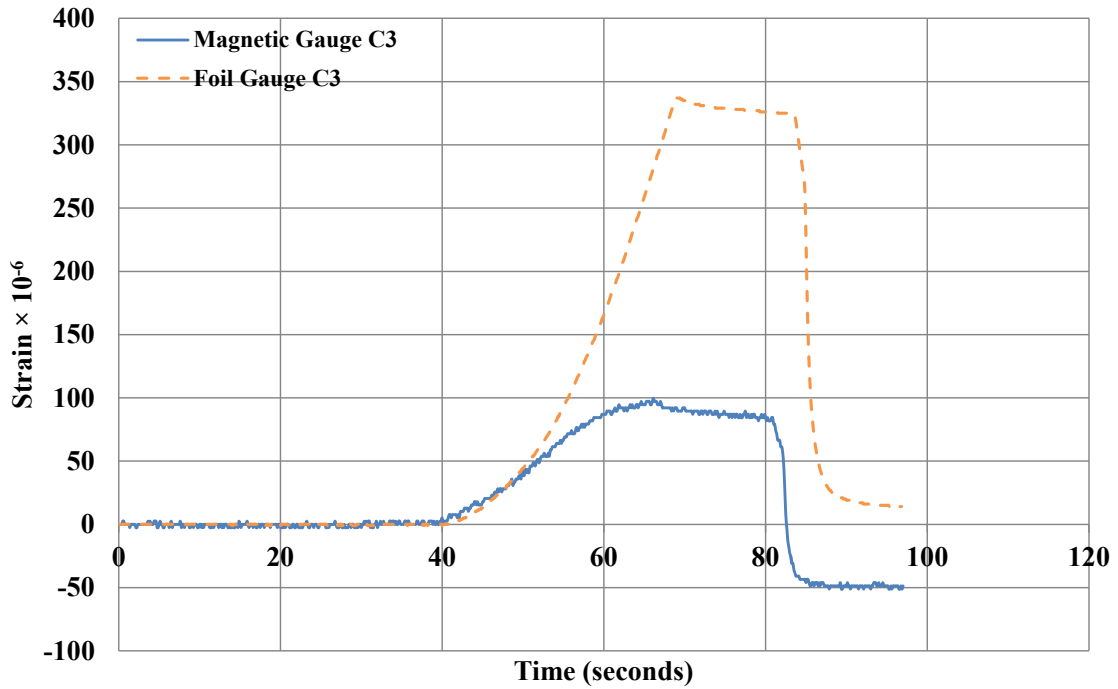
Fig. A14. CFRP Splice Beam Pre Load 3 - C3
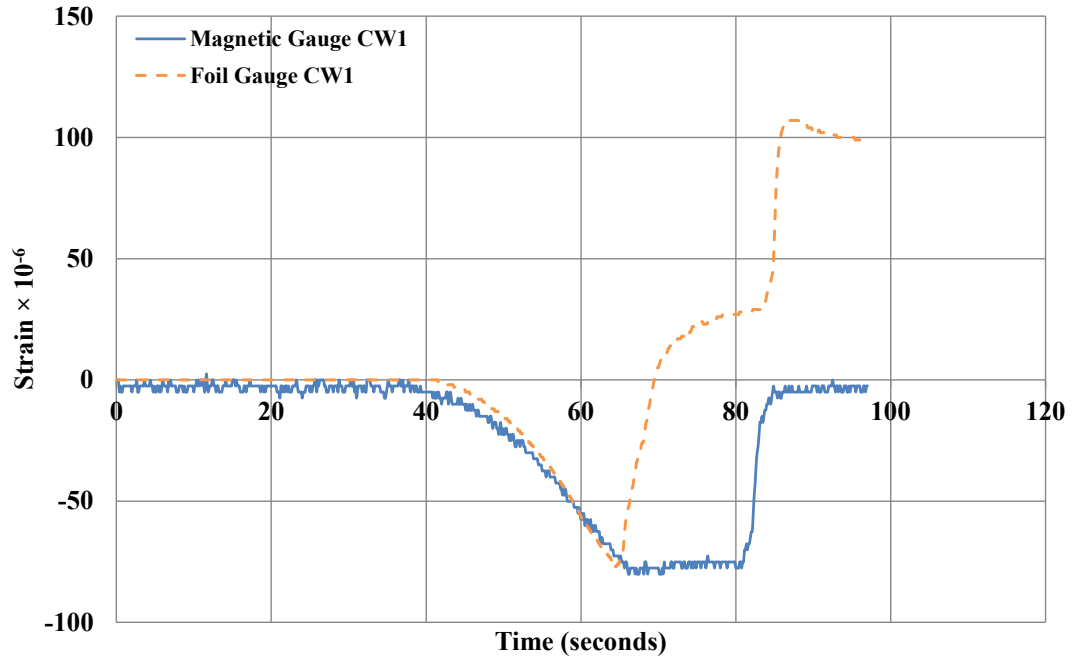
Fig. A15. CFRP splice beam pre load 3 - CW1
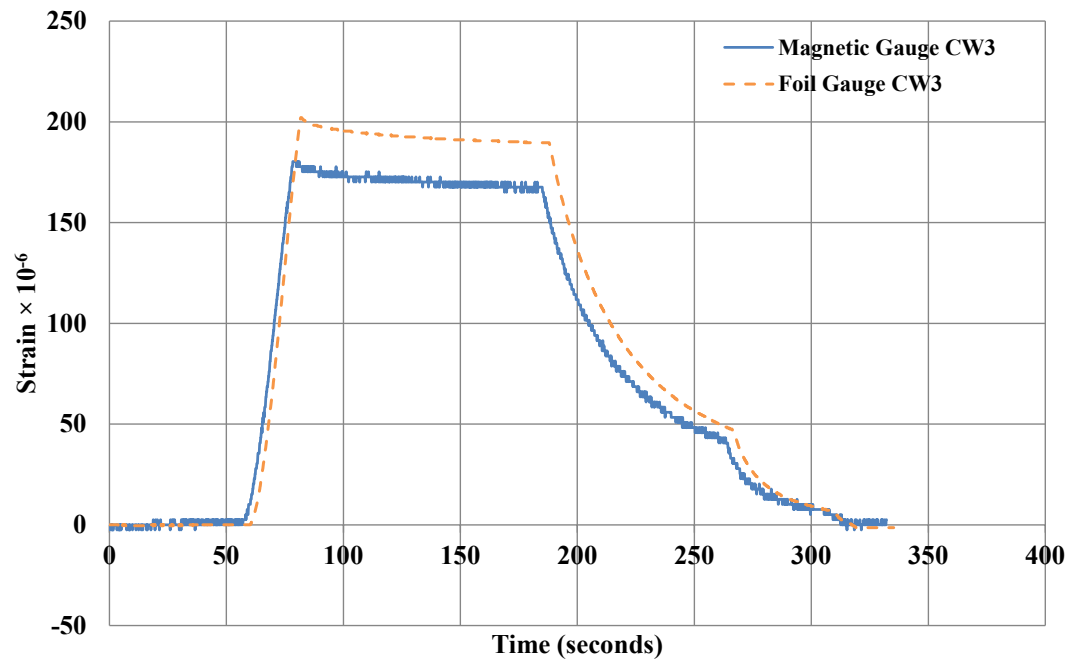
Fig. A16. CatStrong pre load 1 - CW3
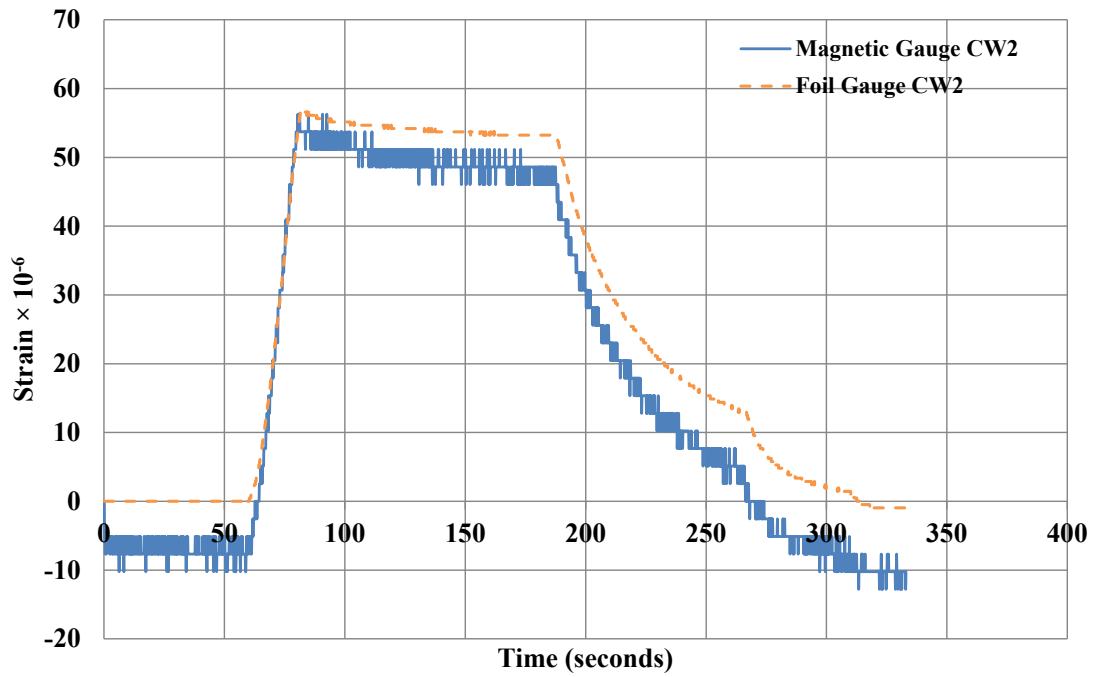
Fig. A17. CatStrong pre load 1 - CW2
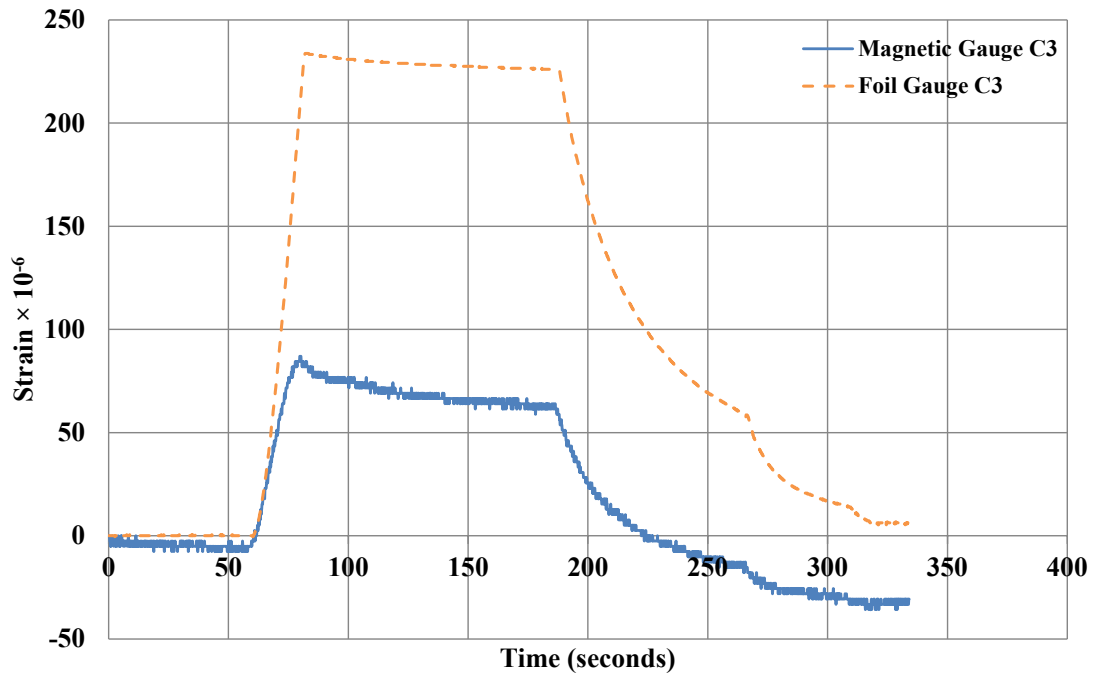
Fig. A18. CatStrong pre load 1 - C3
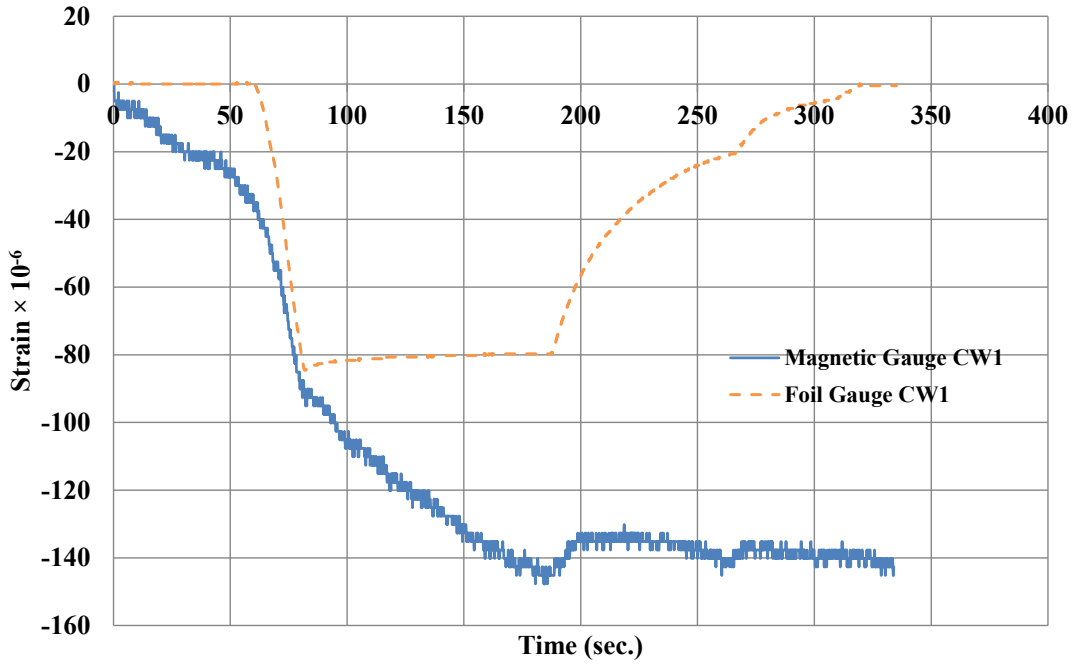
Fig. A19. CatStrong pre load 1 - CW1
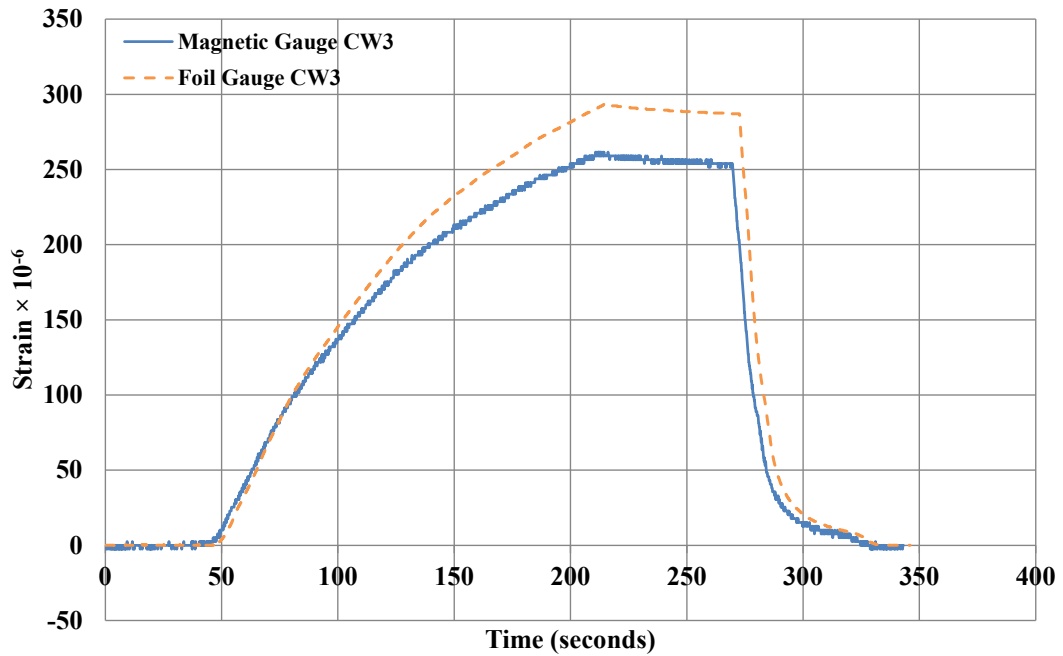
Fig. A20. CatStrong pre load 2 - CW3
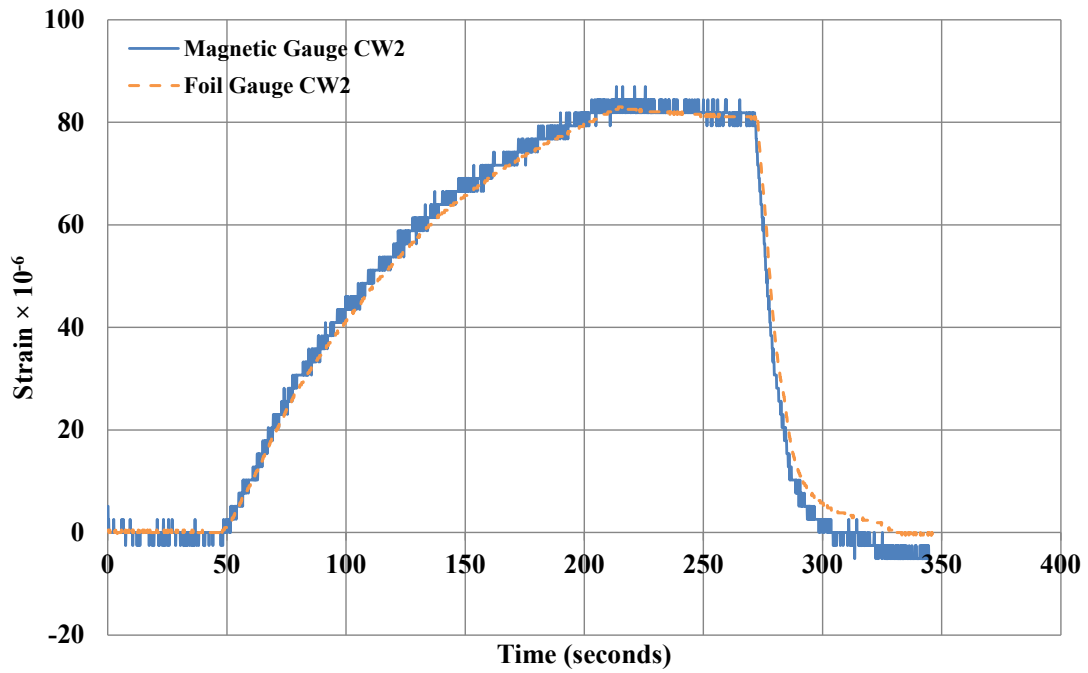
Fig. A21. CatStrong pre load 2 – CW2
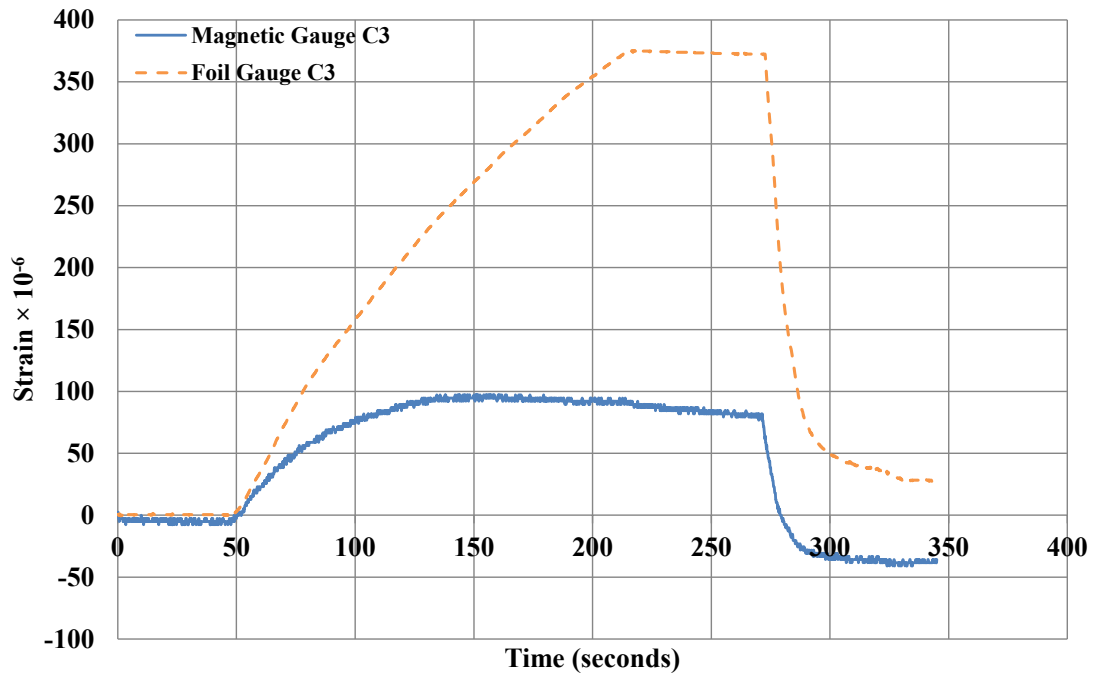
Fig. A22. CatStrong pre load 2 - C3
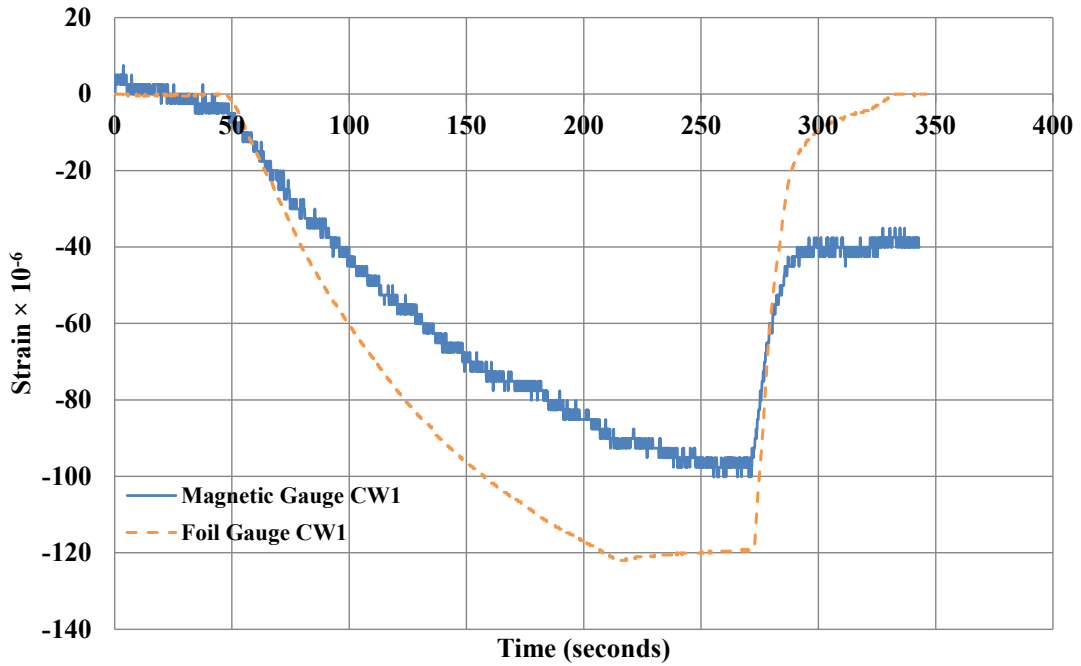
Fig. A23. CatStrong pre load 2 - CW1
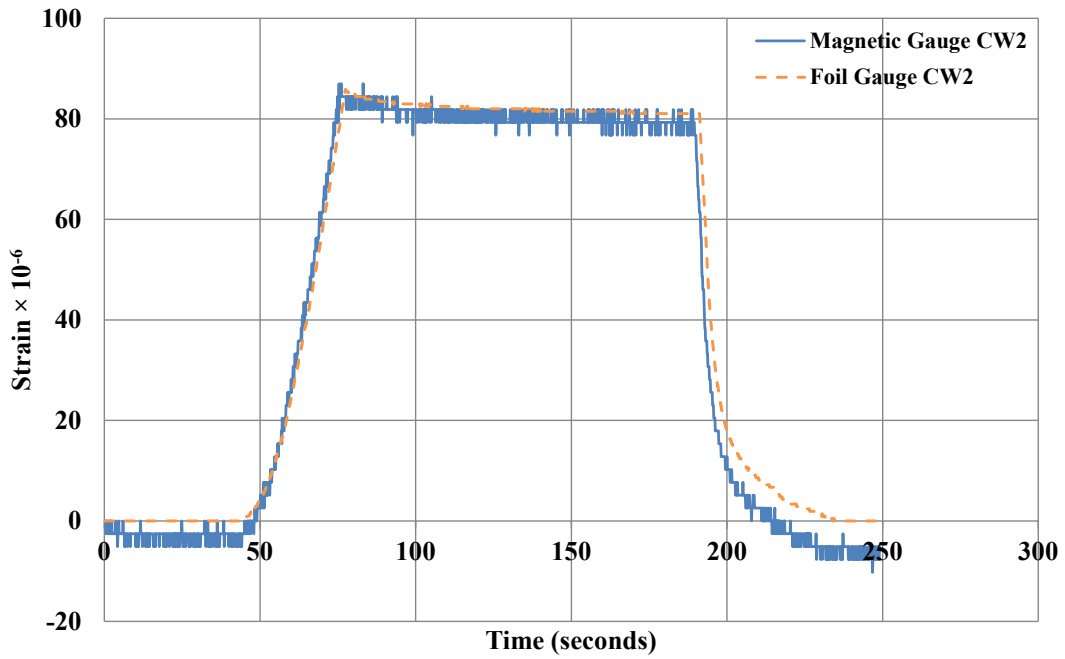
Fig. A24. CatStrong Pre Load 3 - CW2
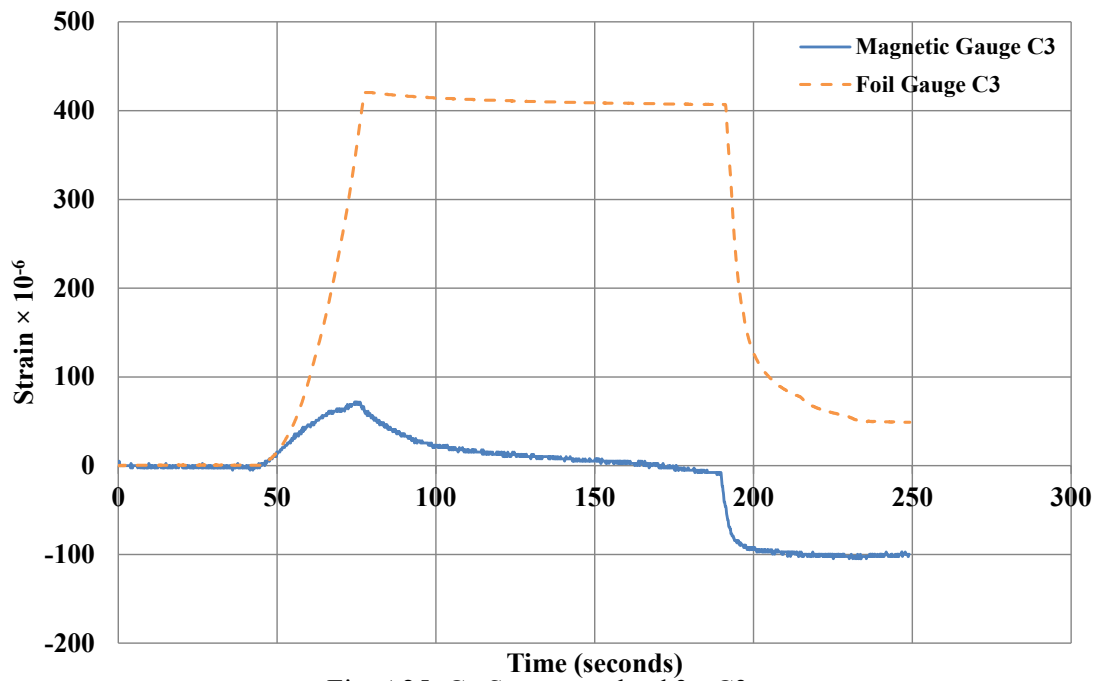
Fig. A25. CatStrong pre load 3 - C3
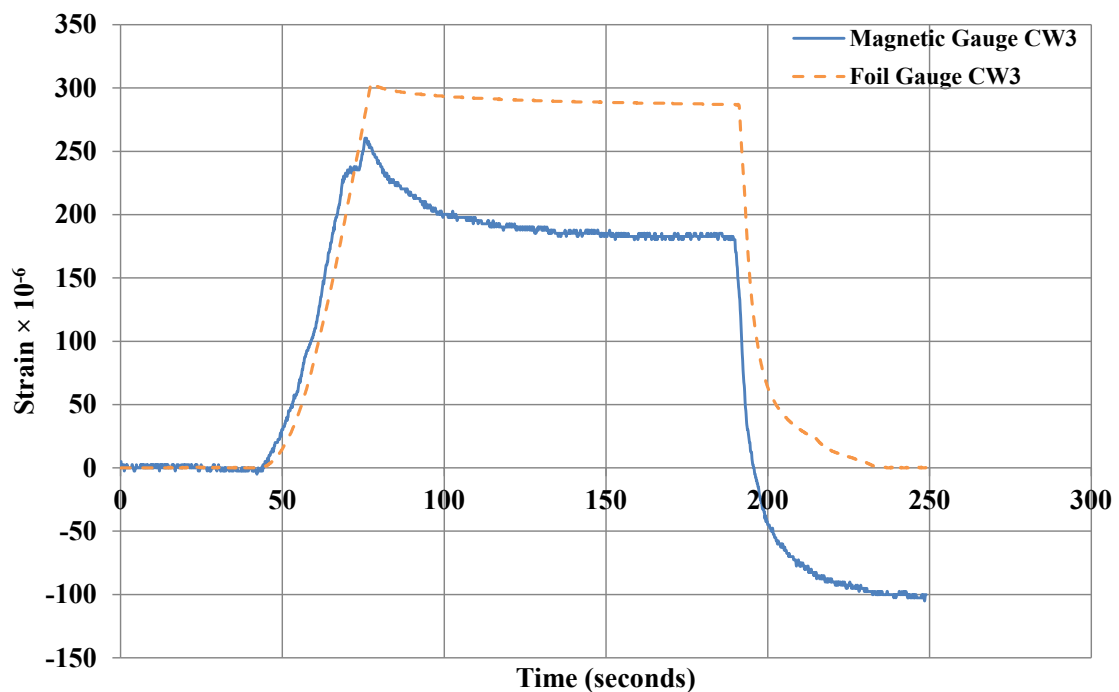
Fig. A26. CatStrong pre load 3 - CW3

Appendix B. AASHTO Load Rating For Lewis County Bridge

Section Properties (W33×130)
Area	A_s	: 38.3	in²
Depth	d	: 33.1	in
Web thickness	t_w	: 0.58	in
Flange width	b_f	: 11.5	in
Flange thickness	t_f	: 0.855	in
Nominal Weight	w_s	: 130	lb/ft
Moment of Inertia	I_{xx}	: 6710	in⁴
Elastic section modulus	S_{xx}	: 406	in³
Plastic section modulus	Z_{xx}	: 467	in³

Material Properties
Modulus of Steel	E_s	: 29000	ksi	
Yield strength	F_y	: 33	ksi	(assumed)
Concrete density	w_c	: 150	pcf	
Concrete strength	f'_c	: 3.5	ksi	

Span Length	L	: 61	ft
Deck height	h_d	: 6.5	in
Effective deck width	b_e	: 6	ft

Check for compact section
AASHTO Standard Specifications 10.48.1

(a) Compression Flange

$$\frac{b_f}{t_f} \leq \frac{4110}{\sqrt{F_y}} \qquad => \qquad 13.45 \leq 22.62 \qquad \text{O.K}$$

(b) Web thickness

$$\frac{D}{t_w} \leq \frac{19230}{\sqrt{F_y}} \qquad => \qquad 54.12 \leq 105.86 \qquad \text{O.K}$$

D= 31.39 in. is the clear distance between the flanges

Nominal Flexural Strength $\quad M_n \quad = F_y Z_{xx}$

$$= 33 \times 467$$

$$= \underline{1284 \text{ kip-ft}}$$

Loads
Deck weight   = 787.5 lb/ft   (includes curb and wearing surface)
Steel Beam Weight   = 130   lb/ft

Total weight $w_T = 787.5 + 130 = 917.5$ lb/ft

Dead load moment M_{DL} $= \dfrac{w_T L^2}{8} =$

$= 426.75$ kip-ft

Impact factor I $= \dfrac{50}{L+125} \leq 0.3$

I $= 0.27$

Distribution factor DF $= S_s/5.5$

$= 6/5.5 = 1.09$

Live and Impact load moments
- Truck Type HS20

Load   per beam P_1 = 16   kips   (½ the center axle weight at mid span)
Live load M_{L1} = 244 kip-ft

Load   per beam P_2 = 16   kips   (½ the rear axle weight 14' from mid span)
Live load M_{L2} = 132 kip-ft

Load   per beam P_3 = 4   kips   (½ the front axle weight 14' from mid span)
Live load M_{L3} = 33   kip-ft

M_L = (244+132+33) × 1.09 = 446   kip-ft

AASHTO Manual for condition evaluation of bridges 6.5.1

$$RF = \dfrac{C - A_1 D}{A_2 L (1+I)}$$

where; RF = Rating Factor for the live-load carrying capacity. The rating factor
                      multiplied by the rating vehicle in tons gives the rating of the structure.
              C = Capacity of member
              D = Dead load effect on member
              L = Live load effect on member
              I = Impact factor to be used with the live load effect
              A_1 = Factor for dead loads
              A_2 = Factor for live loads

A_1 = 1.3 for Inventory and Operating levels
A_2 = 2.17 for Inventory and 1.3 for Operating levels   (AASHTO Manual 6.5.3)

Truck Type HS20
        Inventory level RF = [1284 – (1.3×426.75)]/(2.17×1.27×446)   = 0.594

Operating level RF $= [1284 - (1.3 \times 426.75)]/(1.3 \times 1.27 \times 446)$ $= 0.991$

Appendix C. Lewis County Bridge Load Test Results
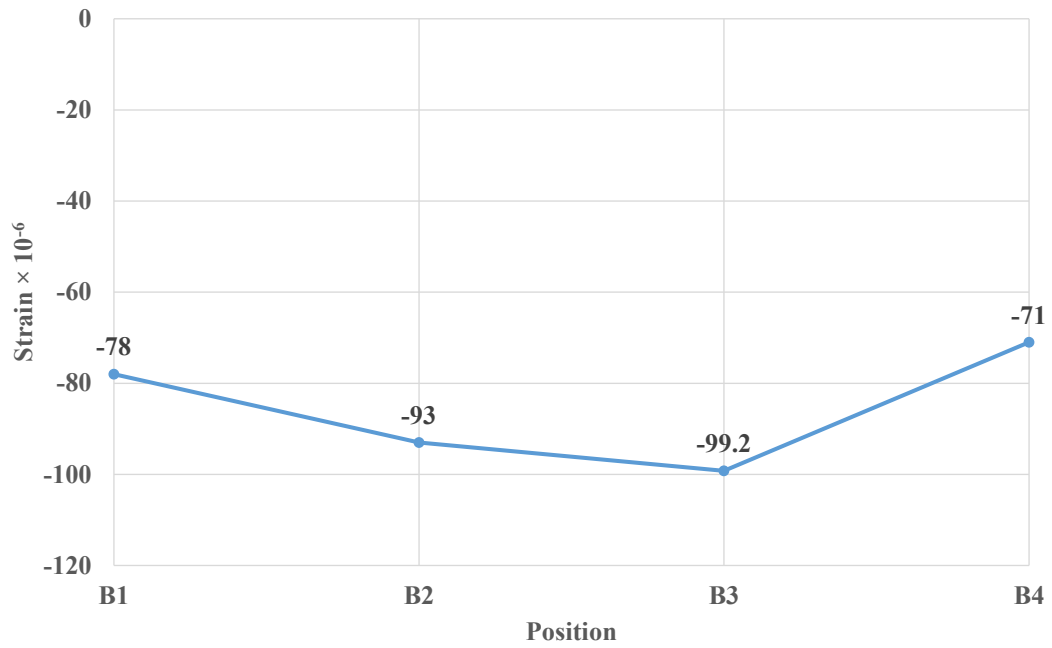
Fig. C1. Load case 1 – s**outh**
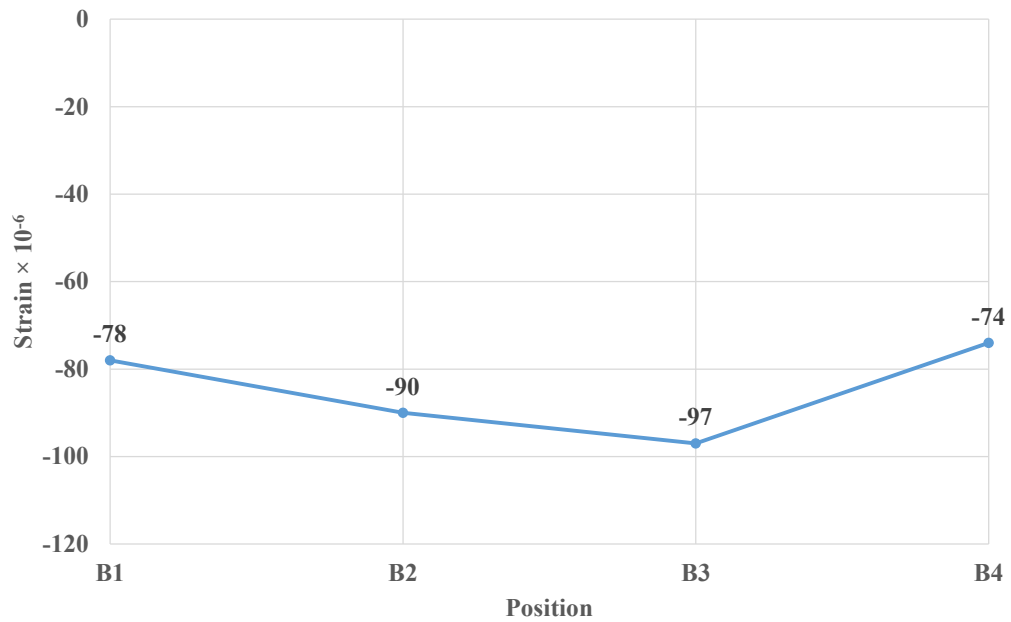
Fig. C2. Load case 1 – north
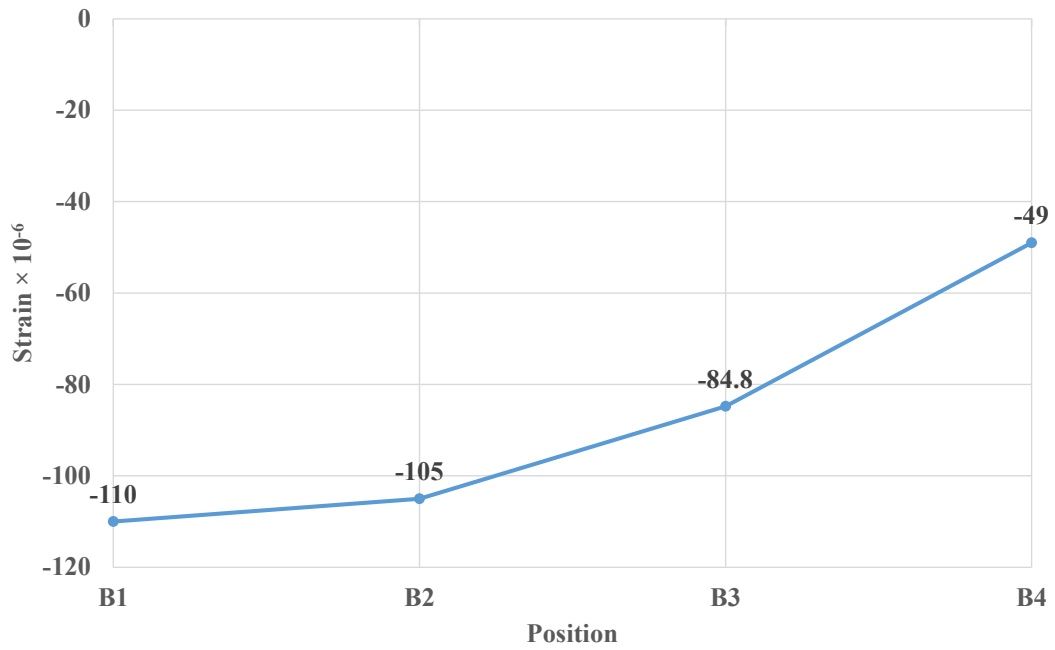
Fig. C3. **Load** case 2 – south
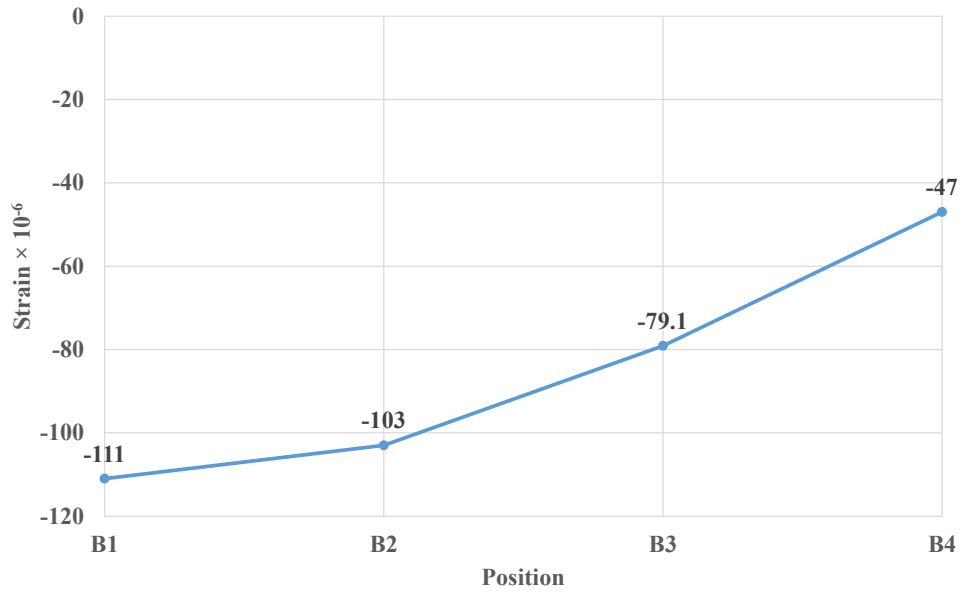
Fig. C4. Load case 2 – north
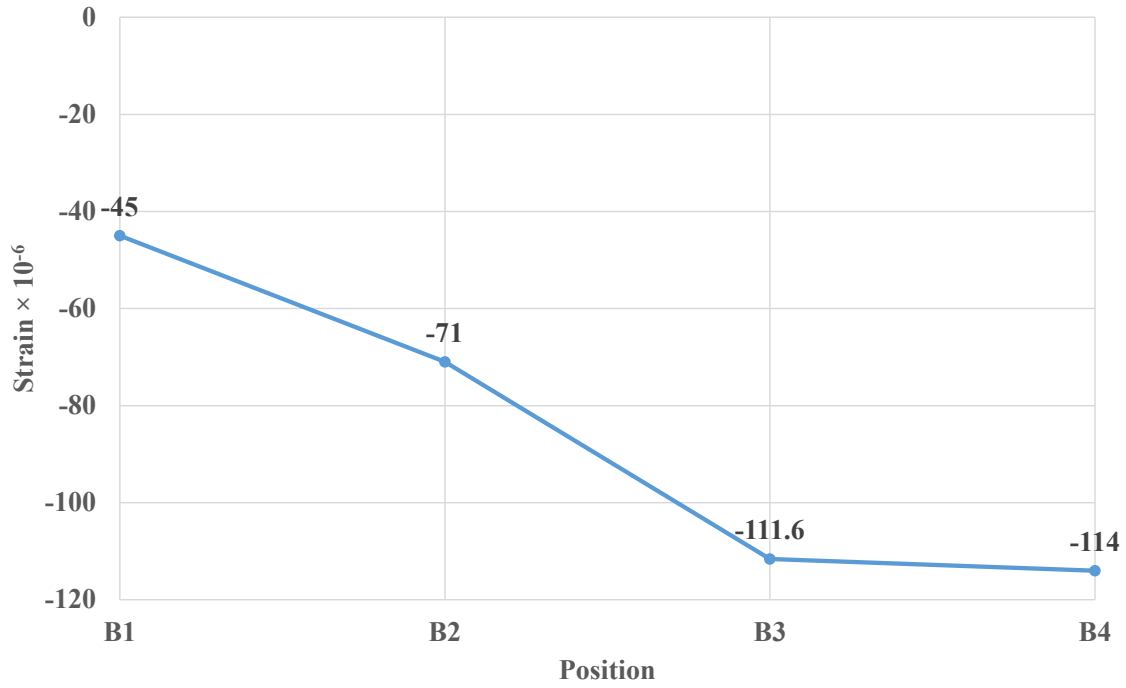
Fig. C5. Load case 3 – south
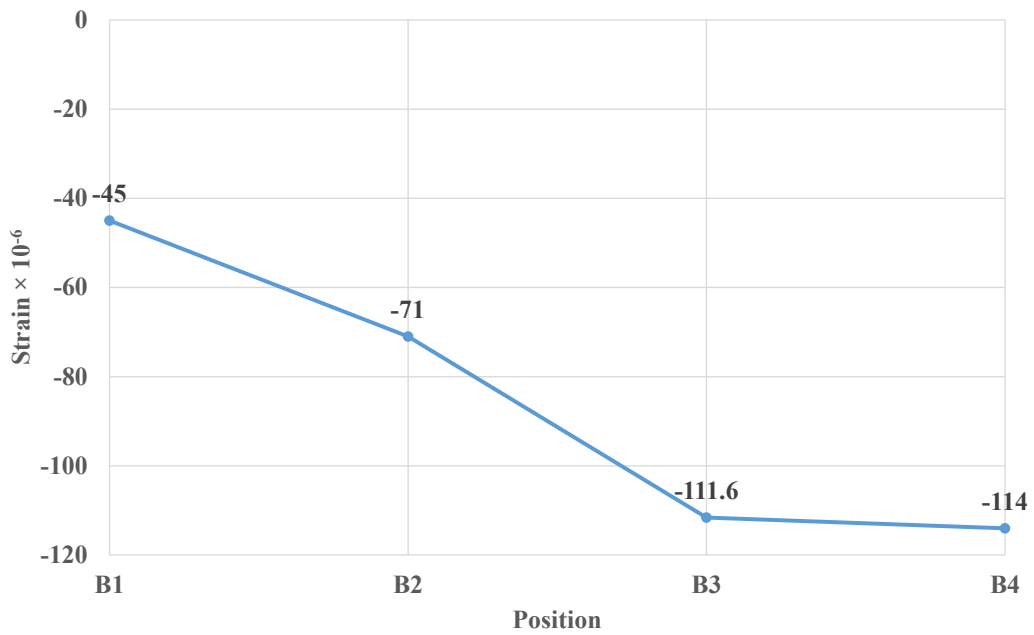
Fig. C6. Load case 3 – north
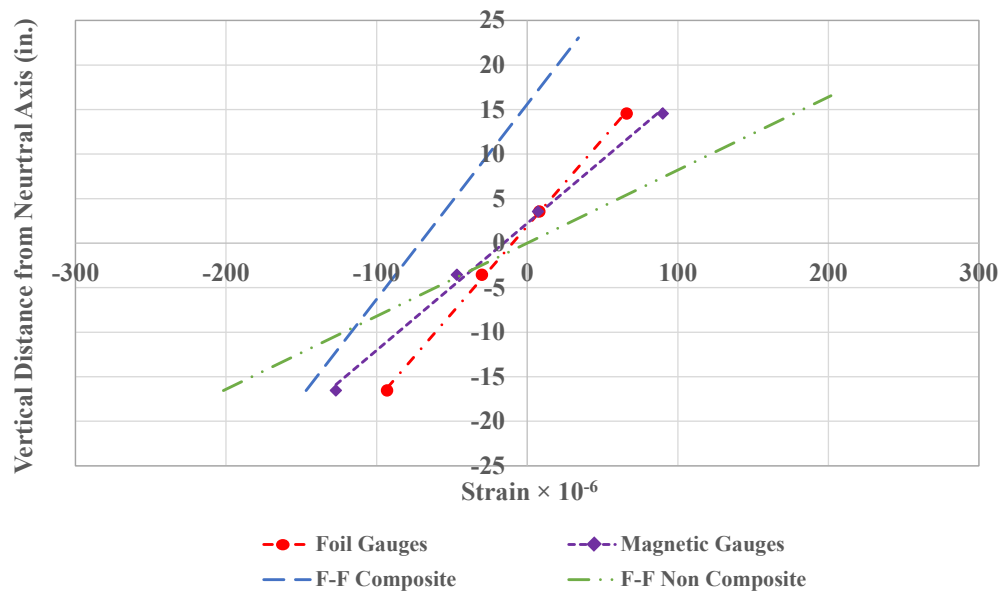
Fig. C7. B2 strain profile – load case 1 – south
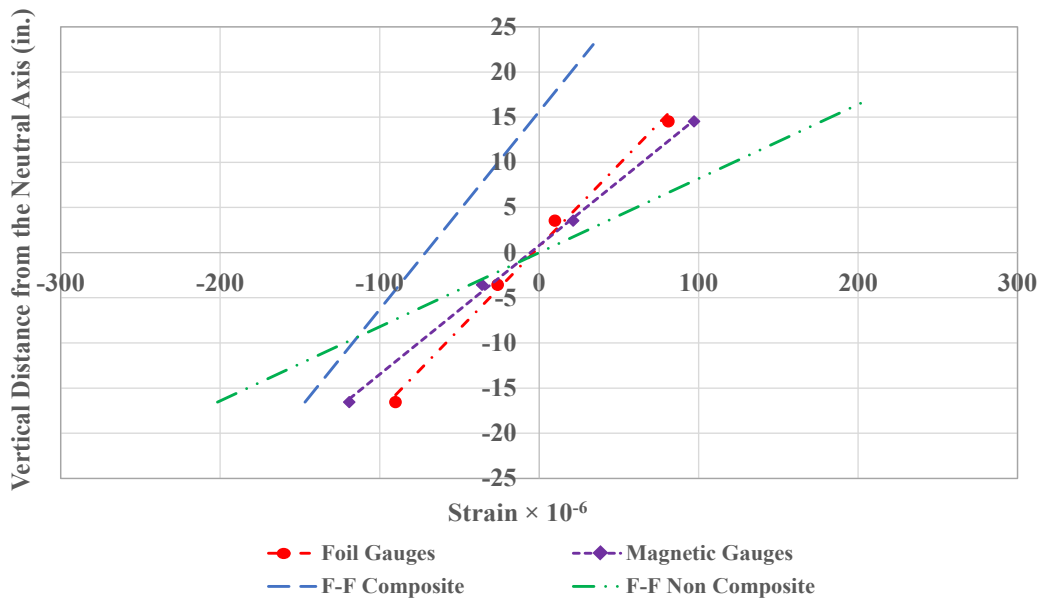
Fig. C8. B2 strain profile – load case 1 – north
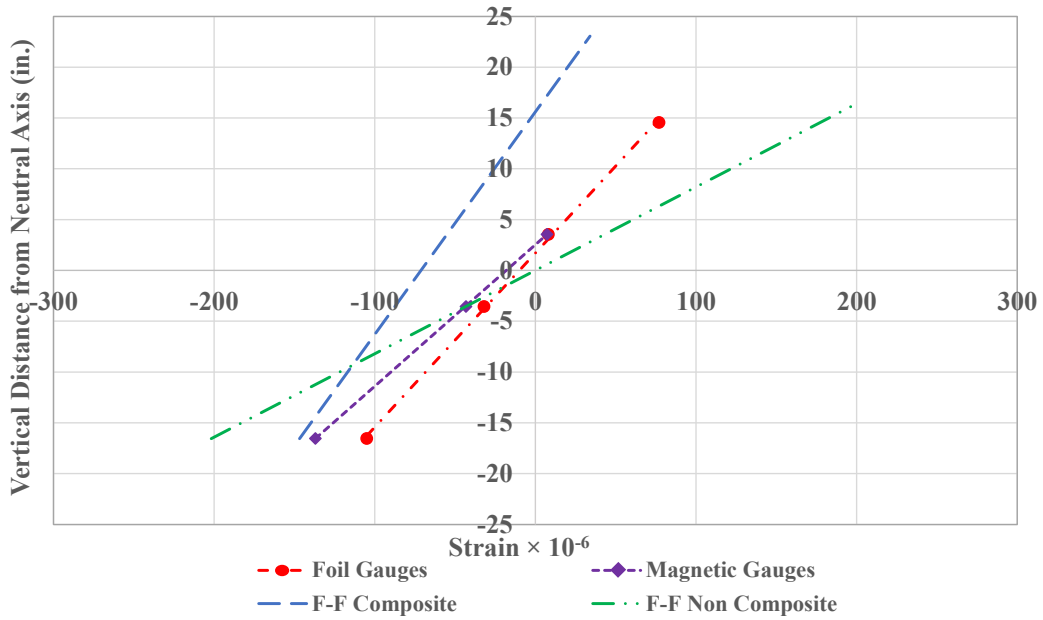
Fig. C9. B2 strain profile – load case 2 – south
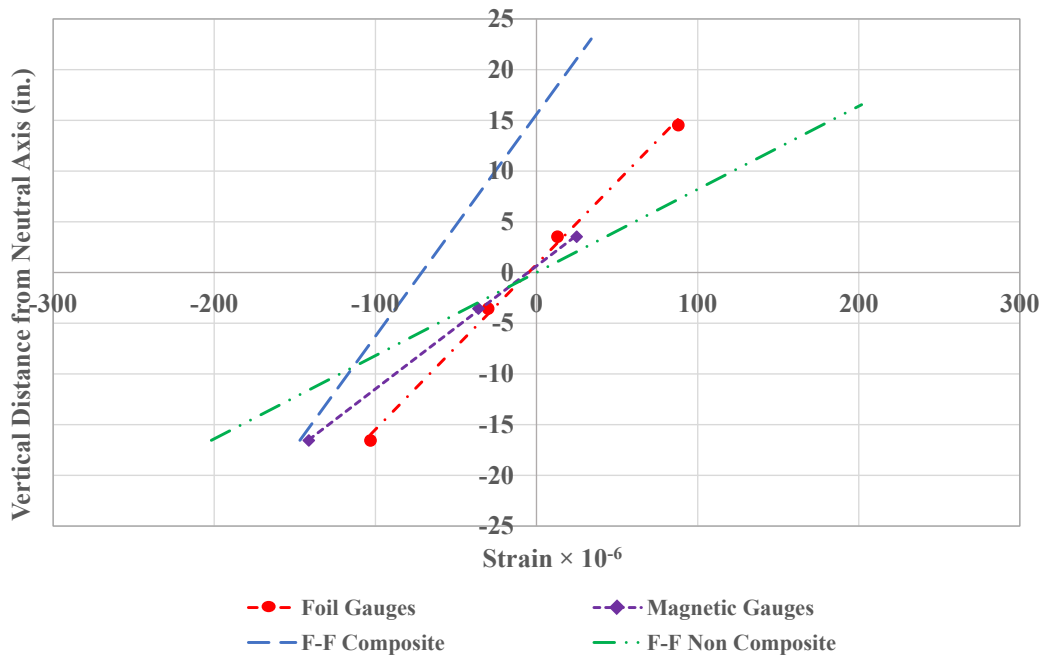
Fig. C10. B2 strain profile – load case 2 – north
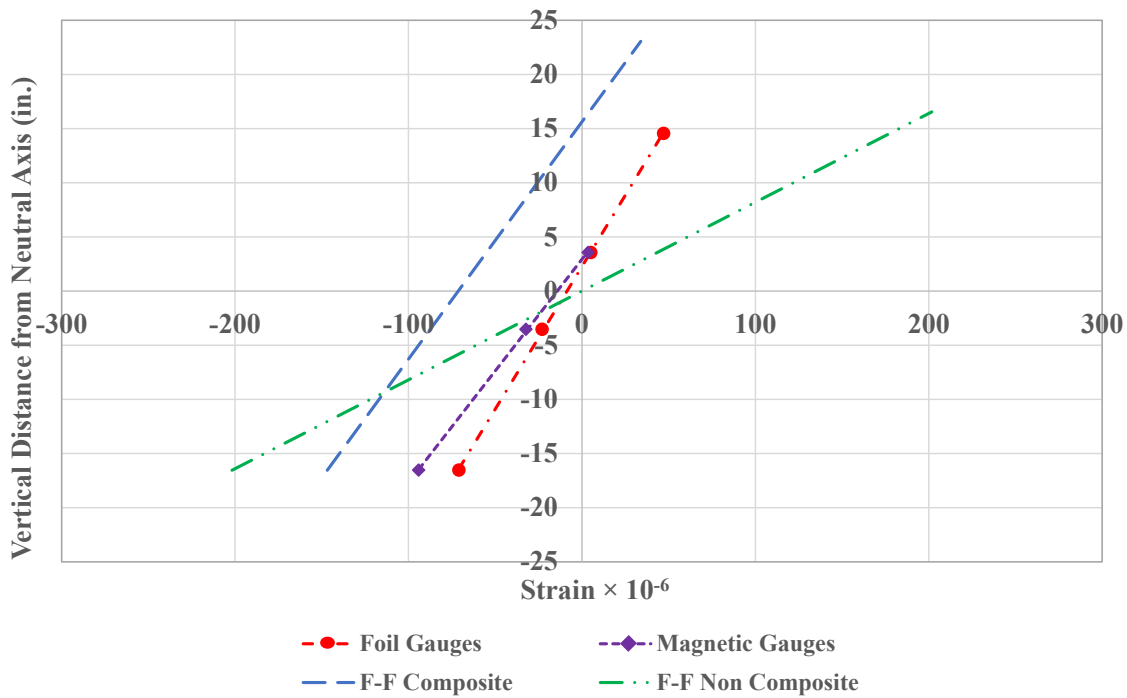
Fig. C11. **B2** strain profile – load case 3 – south
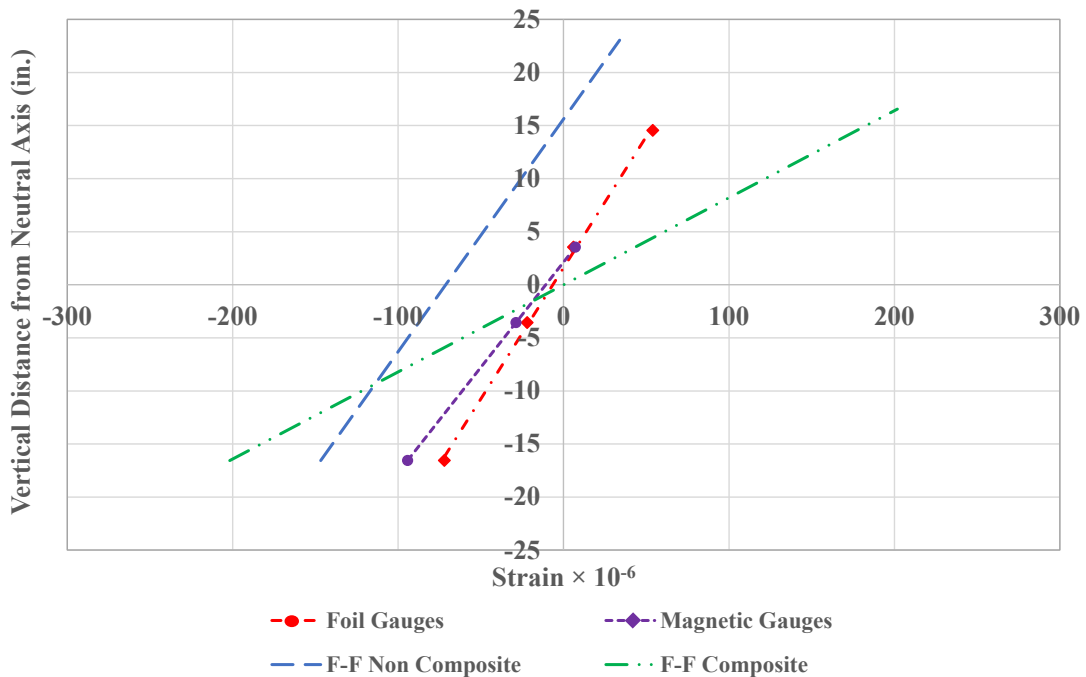
Fig. C12. **B2** strain profile – load case 3 – north

Appendix D. Load Rating Of Lewis County Bridge Through Load Test Results

Field load test Distribution Factor:

$$DF = \sum (\varepsilon_{interior\ beam}/\varepsilon_{all\ beams})$$
$$= 114 / (114+111.6+71+45)$$
$$= 0.334$$

Live load Moment of Test Truck:

Load   per beam $P_1 = 43.44$ kips   (rear axle weight at mid span)
$$M_{L1} = 662.46 \text{ kip-ft}$$

Load   per beam $P_2 = 18.26$ kips   (front axle weight 14' from mid span)
$$M_{L2} = 132.38 \text{ kip-ft}$$

$$M_L = (662.46+132.38) \times 0.334 = 264.68 \text{ kip-ft}$$

The maximum strain due to M_L:

$$\varepsilon_c = M_L/(E \times S_x)$$
$$= 264.68 \times 12 /(29{,}000 \times 406)$$
$$= 270 \text{ microstrains}$$

$$\varepsilon_T = 159 \text{ microstrains (from field test readings)}$$

Therefore from NCHRP *Manual for Bridge Rating through Load Testing* Eq. (6-4)

$$K_a = (\varepsilon_c/\varepsilon_T) - 1$$
$$= (270/159) - 1 = 0.7$$

From NCHRP *Manual for Bridge Rating through Load Testing* Eq. (6-6)

$$K_b = K_{b1} \times K_{b2} \times K_{b3}$$
$$= 1 \times 0.8 \times 1 = 0.8$$

From **NCHRP Manual for Bridge Rating through Load Testing** Eq. (6-3)
$$K = 1 + K_a \times K_b$$
$$= 1 + (0.7 \times 0.8) = 1.56$$

Truck Type HS20 (from calculations in Appendix A)
Inventory level $RF = 0.594$
Operating level $RF = 0.991$

From **NCHRP Manual for Bridge Rating through Load Testing** Eq. (6-1)
$RF_T = RF \times K$

Inventory level $RF_T = 0.594 \times 1.56 = 0.92$
Operating level $RF_T = 0.991 \times 1.56 = 1.54$

Appendix E. BDI Reusable Strain Gauge Test Results
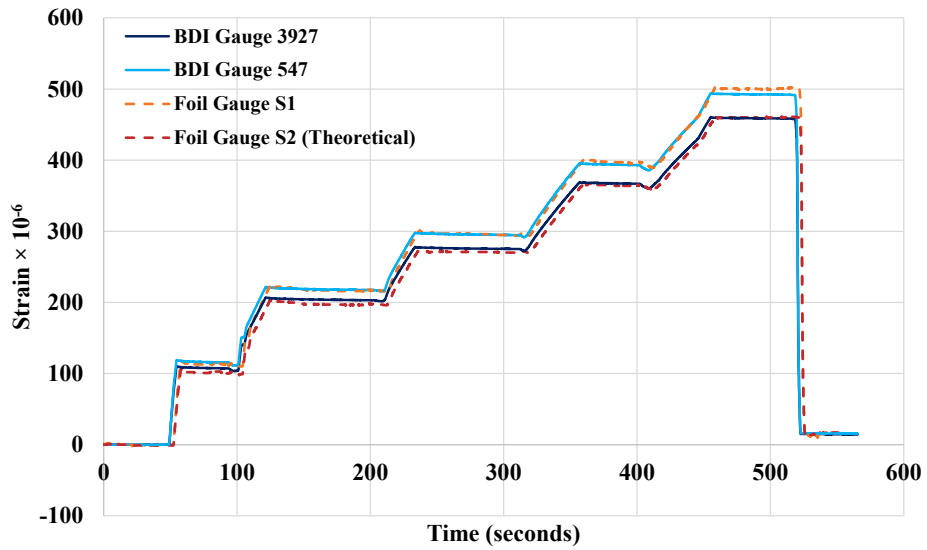
Fig. E1. Beam test 1
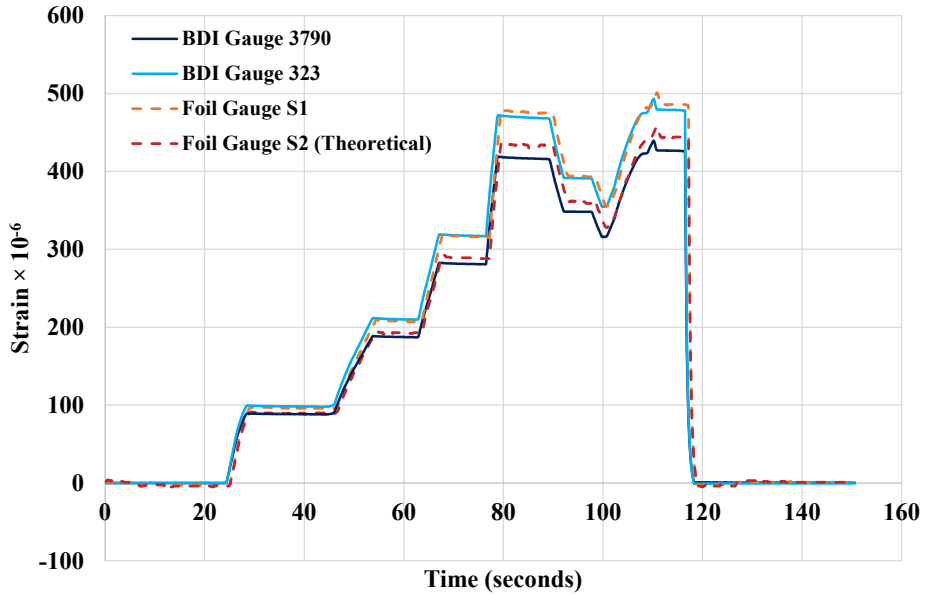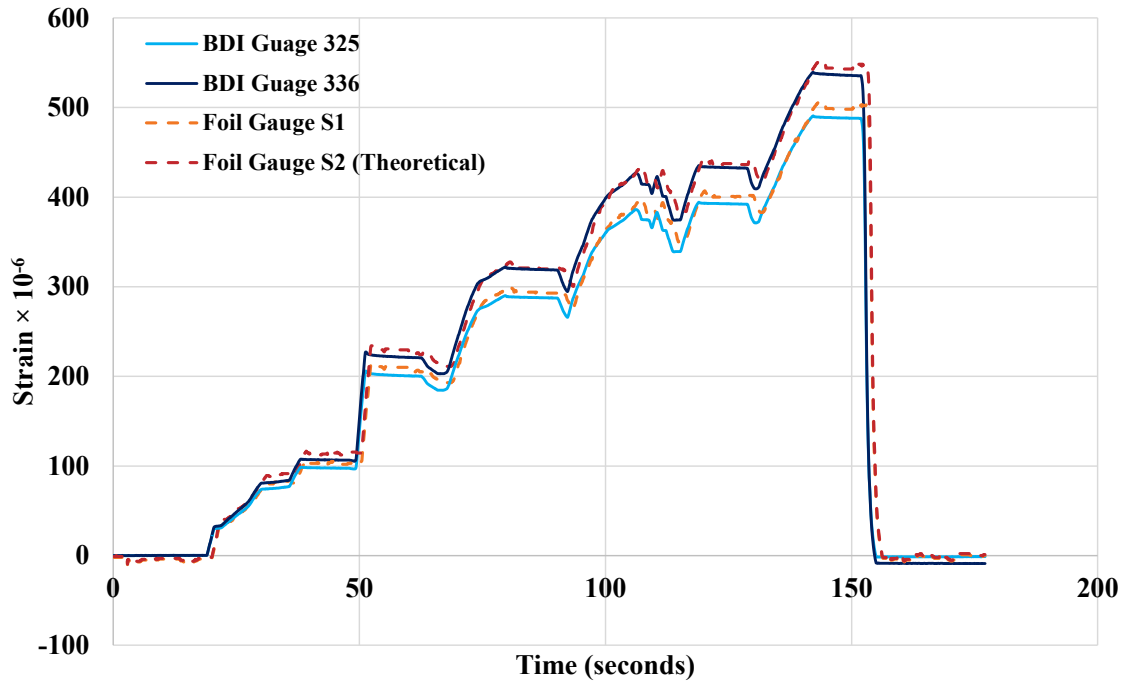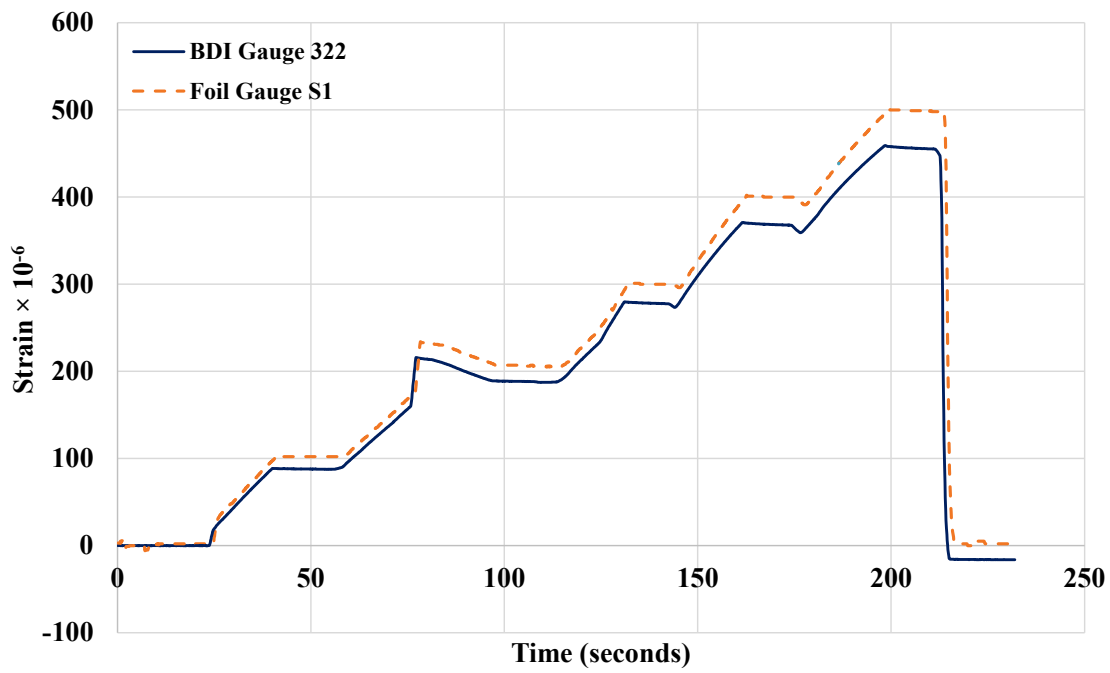
Fig. E2. Beam test 2
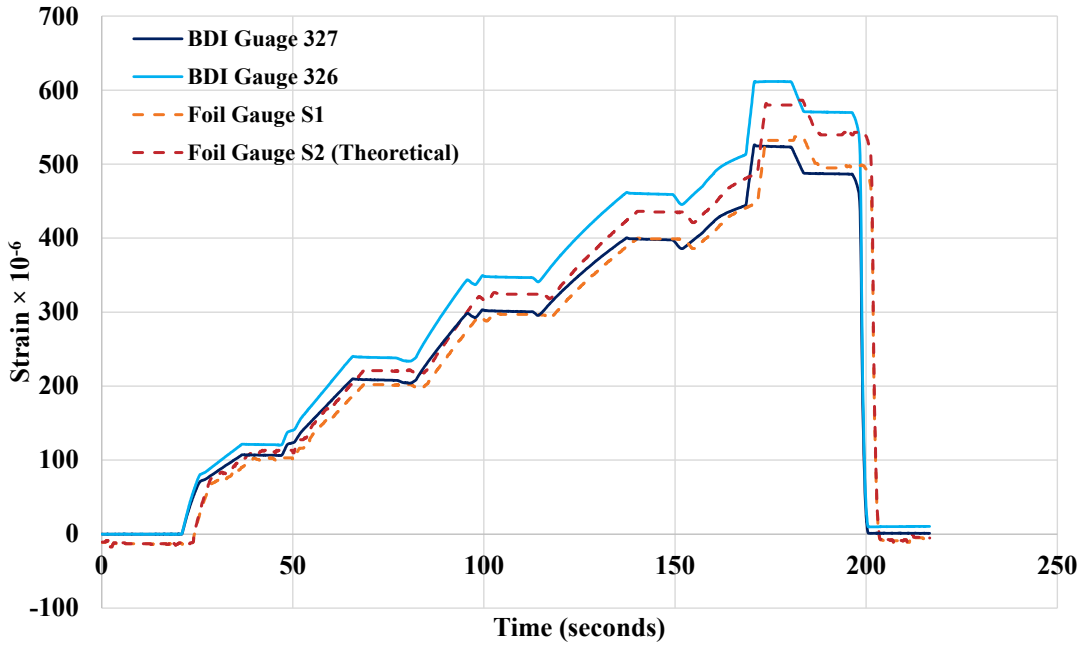
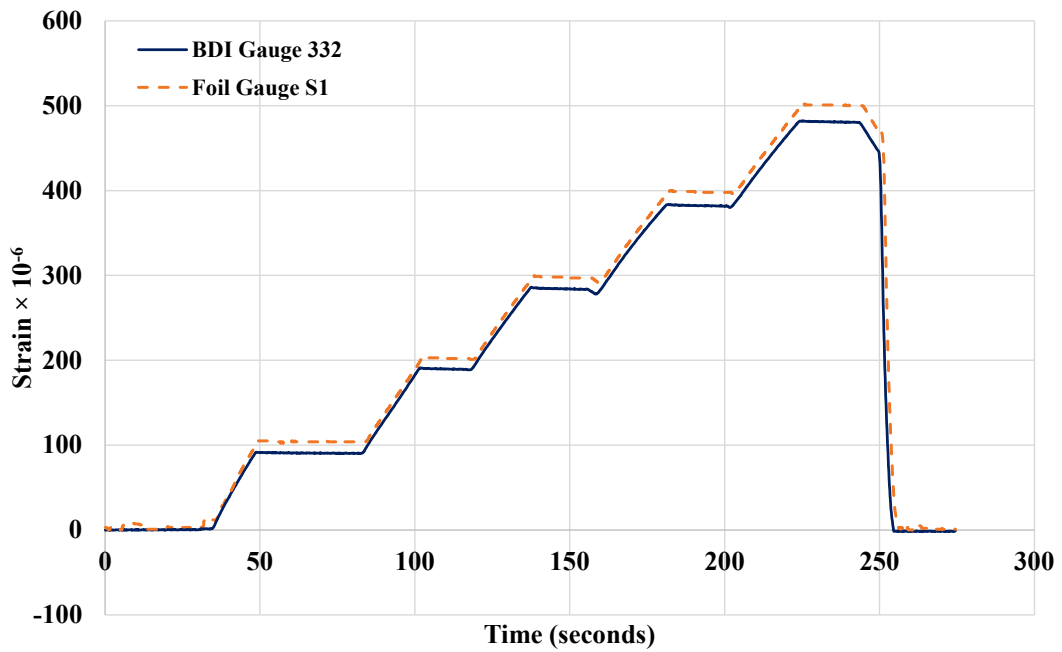

Fig. E3. Beam test 3
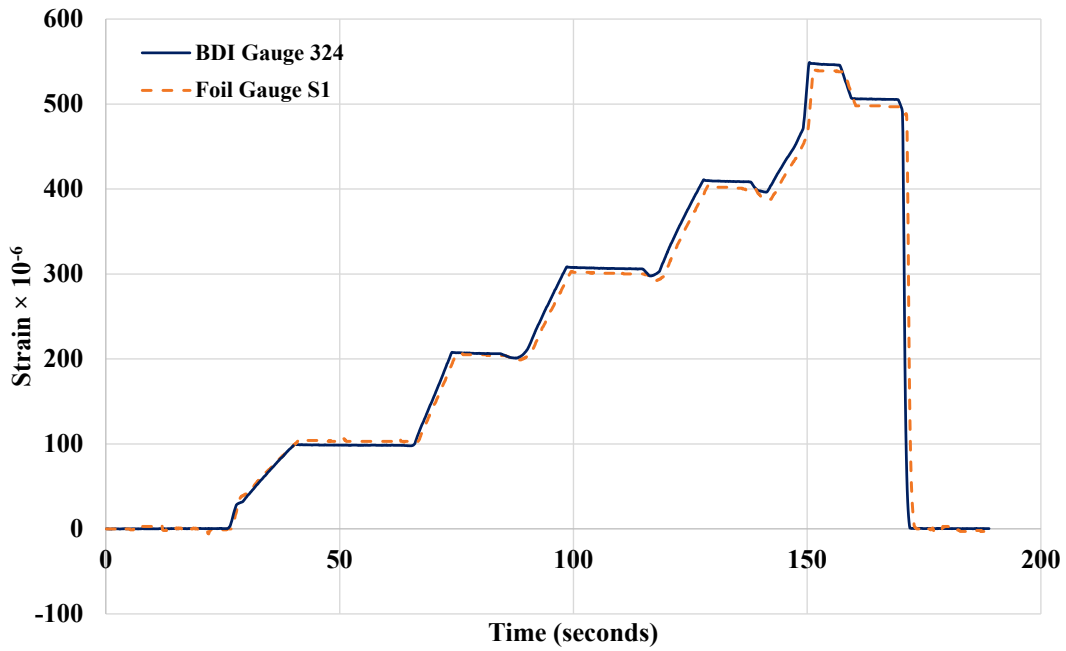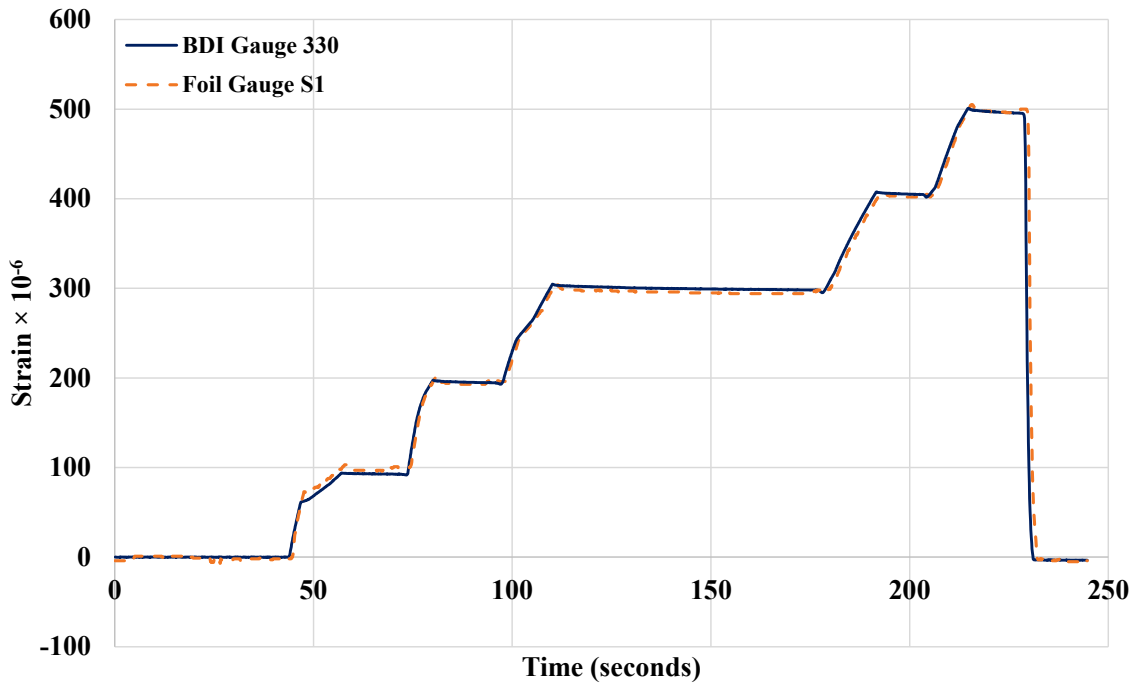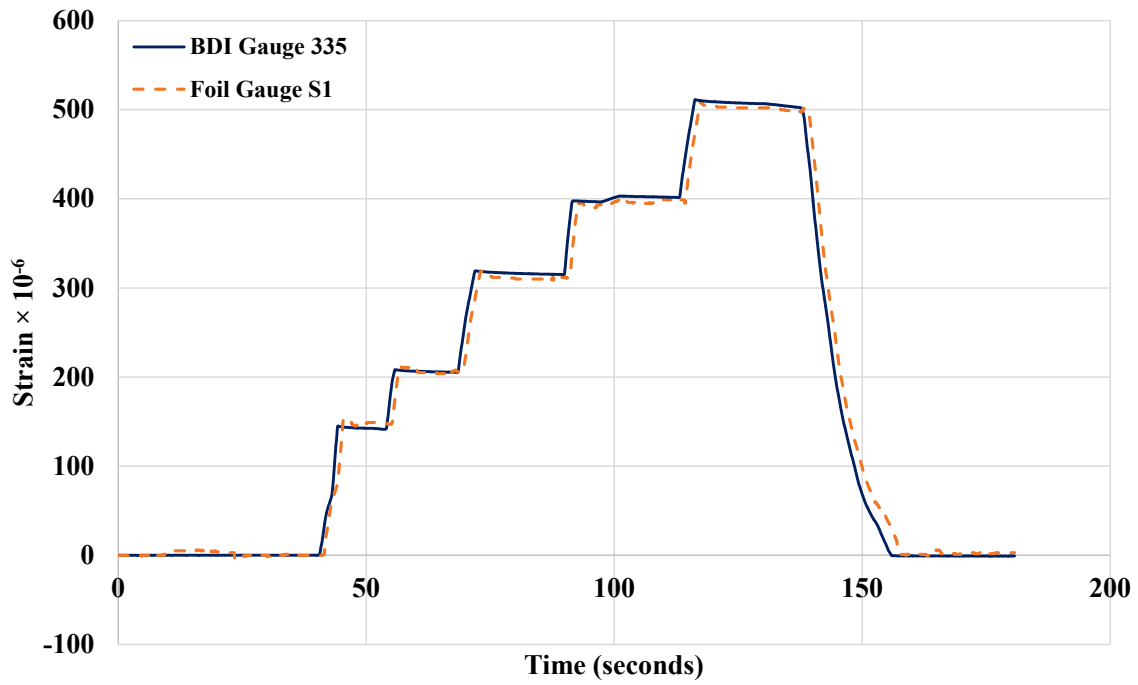

Fig. E4. Beam test 4

Fig. E5. Beam t**est 5**

Fig. E6. Beam t**est 6**

Fig. E7. Beam t**est 7**

Fig. E8. Beam test 8
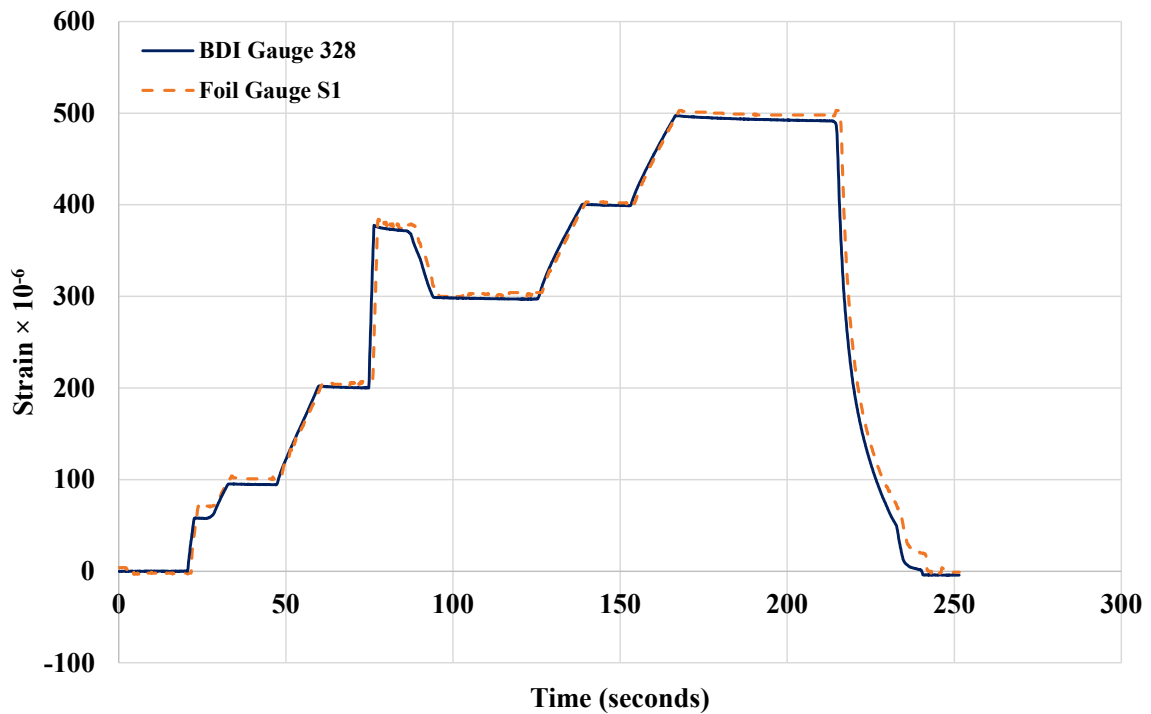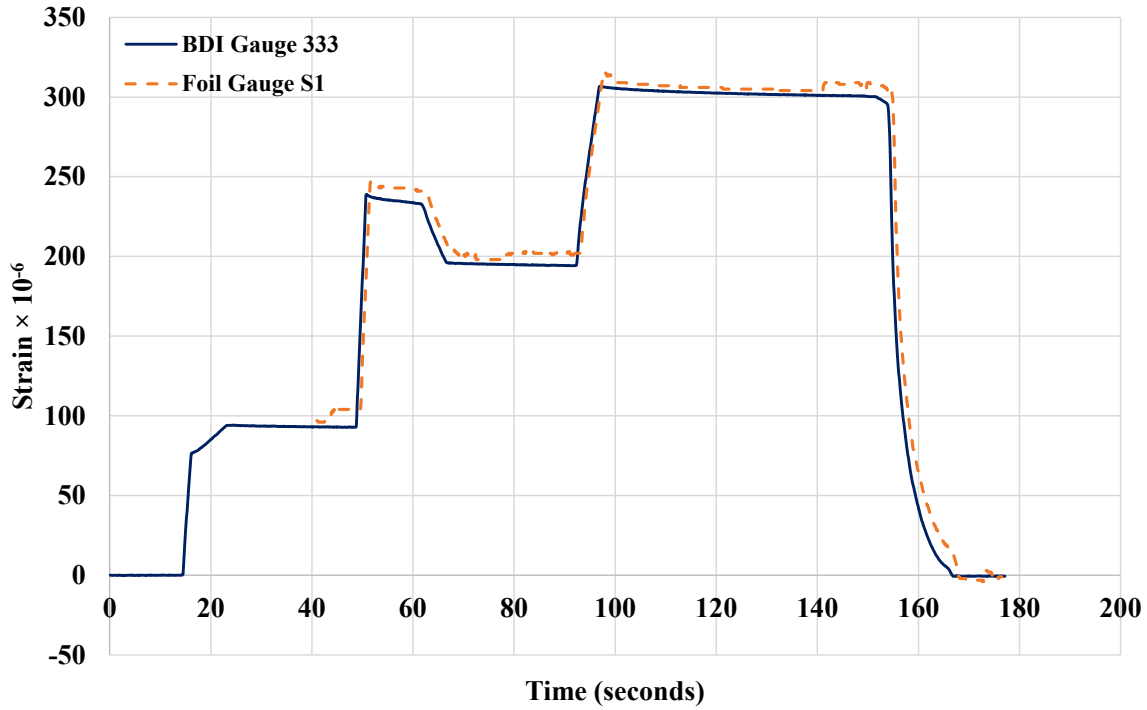

Fig. E9. **Beam t**est 9
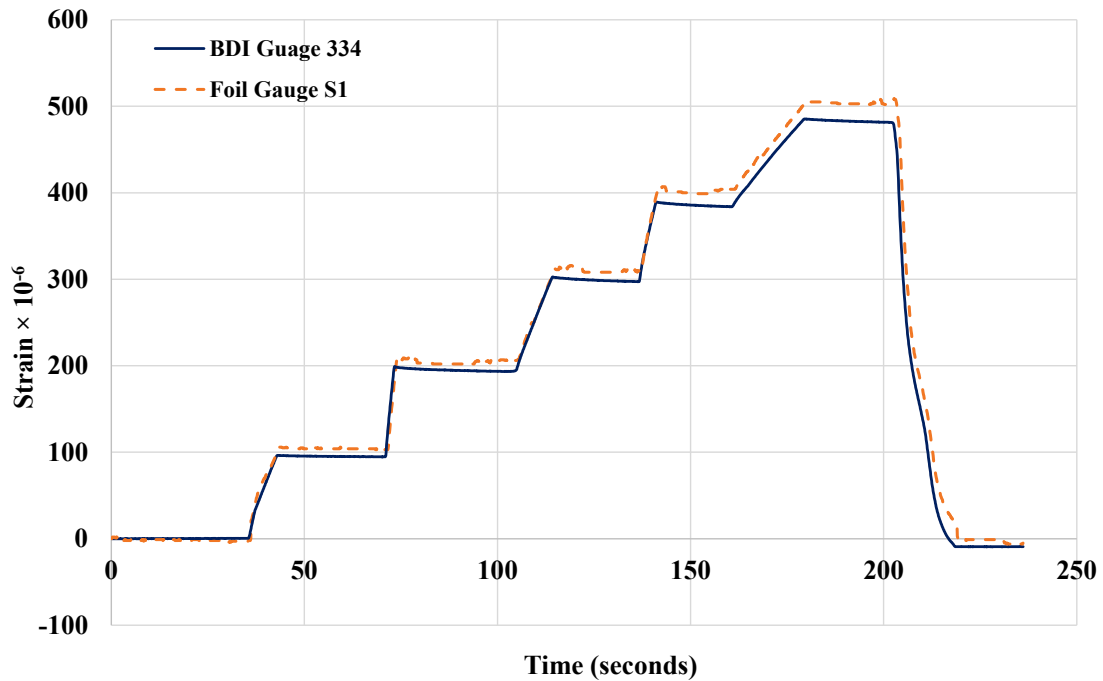

Fig. E10. **Beam t**est 10

Fig. E11. Beam test 11

Fig. E12. Beam Test 12

Appendix F. AASHTO Load Rating For Hardin County Bridge

Section Properties (W18×50)

Area	A_s	: 14.7 in²
Depth	d	: 18.0 in
Web thickness	t_w	: 0.355 in
Flange width	b_f	: 7.50 in
Flange thickness	t_f	: 0.570 in
Nominal Weight	w_s	: 50 lb/ft
Moment of Inertia	I_{xx}	: 800 in⁴
Elastic section modulus	S_{xx}	: 88.9 in³
Plastic section modulus	Z_{xx}	: 101 in³
Plastic Limiting Length	L_p	: 7.17 ft (Calculated using AISC Spec Eq. F2-5)
Elastic Limiting Length	L_r	: 22.2 ft (Calculated using AISC Spec Eq. F2-6)

Material Properties

Modulus of Steel	E_s	: 29000	ksi
Yield strength	F_y	: 33	ksi (assumed)
Concrete density	w_c	: 150	pcf
Concrete strength	f'_c	: 2500	psi

Span Length	L	: 24.67 ft
Deck height	h_d	: 7.0 in

Check for compact section
AASHTO Standard Specifications 10.48.1

(c) Compression Flange

$$\frac{b_f}{t_f} \le \frac{4110}{\sqrt{F_y}} \quad => \quad 13.16 \le 22.62 \quad \text{O.K}$$

(d) Web thickness

$$\frac{D}{t_w} \le \frac{19230}{\sqrt{F_y}} \quad => \quad 47.49 \le 105.86 \quad \text{O.K}$$

D= 16.86 in. is the clear distance between the flanges

Nominal Flexural Strength

$$M_n = C_b \left[M_p - \left(M_p - 0.7 f_y S_{xx} \right) \left(\frac{L_b - L_p}{L_r - L_p} \right) \right]$$

$$M_n = (1) \left[277.75^{k-ft} - (277.75k' - 0.7(33000ksi)(88.9in^3)) \left(\frac{1}{12} \right) \left(\frac{8'-7.17'}{22.2'-7.17'} \right) \right]$$

$$M_n = 272k'$$

Loads
SDL = 823.6 lb/ft   (includes concrete, wearing surface, guardrail, and diaphragm members)
Steel Beam Weight = 50 lb/ft
Total weight w_T = 823.6 + 50 = 873.6 lb/ft

Dead load moment M_{DL} $= \dfrac{w_T L^2}{8} =$
$= 66.5$ kip-ft

Impact factor
$I = \dfrac{50}{125+L} < 0.3$
$I = \dfrac{50}{125+24.67'} < 0.3$
$I = 0.33 < 0.3$
Use $I = 0.3$

Distribution factor DF $= S_s/5.5$

$= 4/5.5 = 0.727$

Live and Impact load moments
- Truck Type HS20
  Load per beam P_1 = 16 kips   (½ the center axle weight at mid span)
  Live load M_{L1} $= 98.7$ kip-ft

  M_L $= (98.7) \times 0.727 = 71.8$ kip-ft

AASHTO Manual for condition evaluation of bridges 6.5.1
$$RF = \dfrac{C - A_1 D}{A_2 L (1+I)}$$
where; RF = Rating Factor for the live-load carrying capacity. The rating factor
            multiplied by the rating vehicle in tons gives the rating of the structure.
        C = Capacity of member
        D = Dead load effect on member
        L = Live load effect on member
        I = Impact factor to be used with the live load effect
        A_1 = Factor for dead loads
        A_2 = Factor for live loads

A_1 = 1.3 for Inventory and Operating levels
A_2 = 2.17 for Inventory and 1.3 for Operating levels   (AASHTO Manual 6.5.3)

Truck Type HS20

Inventory level RF = [272 – (1.3×66.5)]/(2.17×1.3×71.8) = 0.916
Operating level RF = [272 – (1.3×66.5)]/(1.3×1.3×71.8) = 1.529
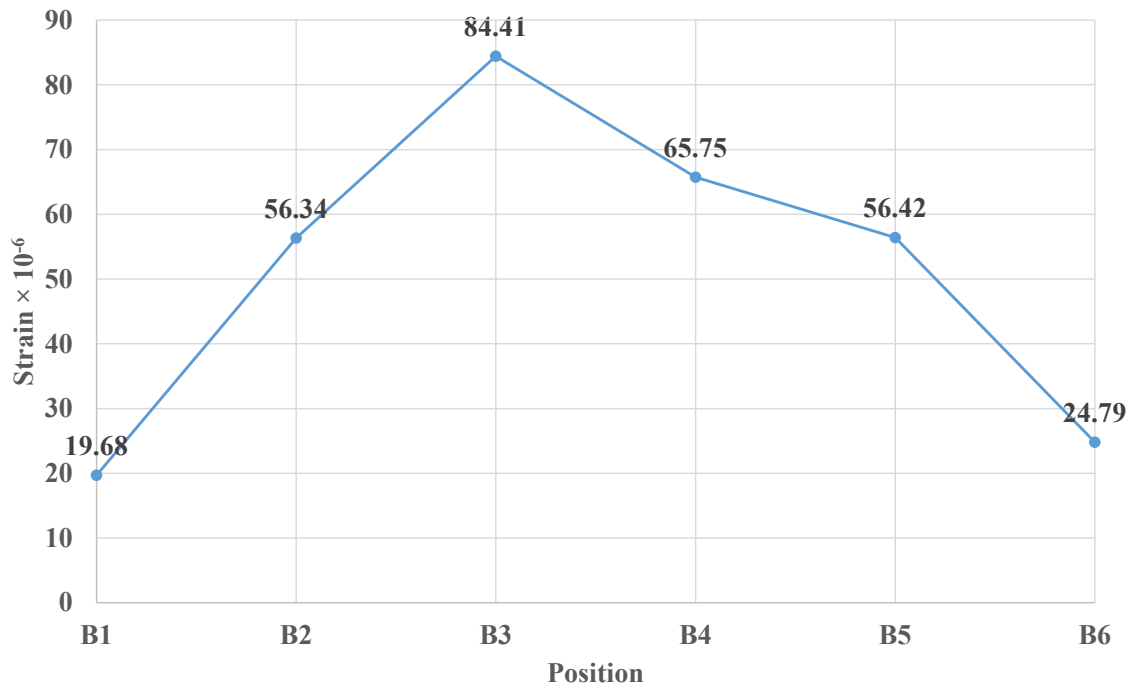
Appendix G. Hardin County Bridge Load Test Results

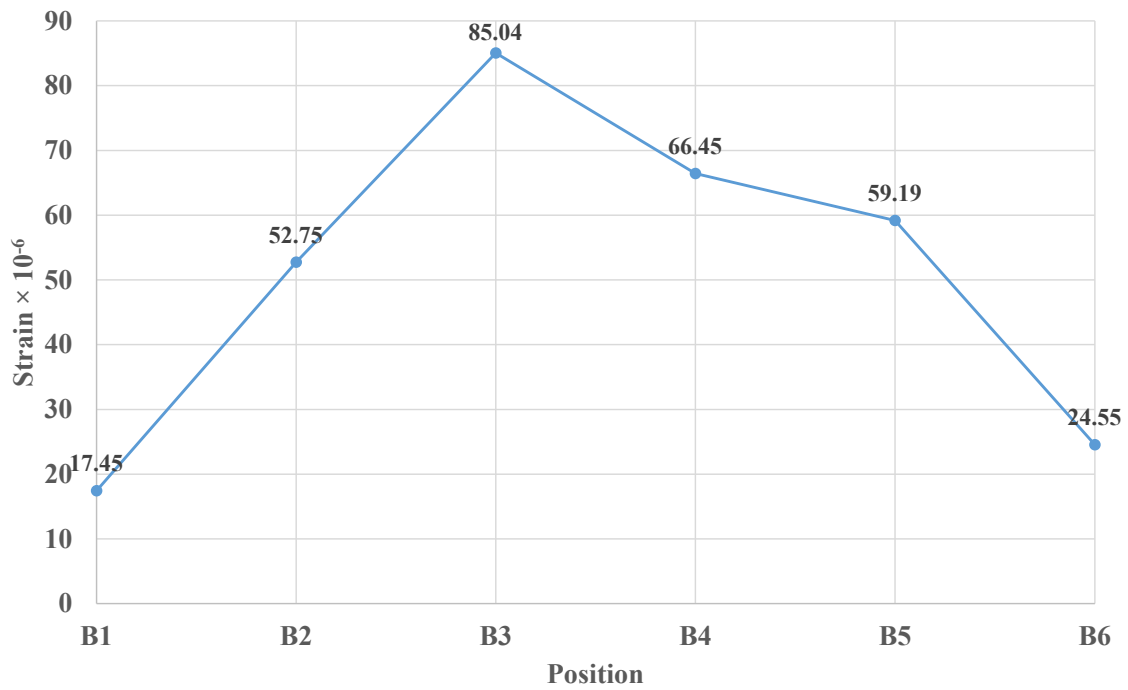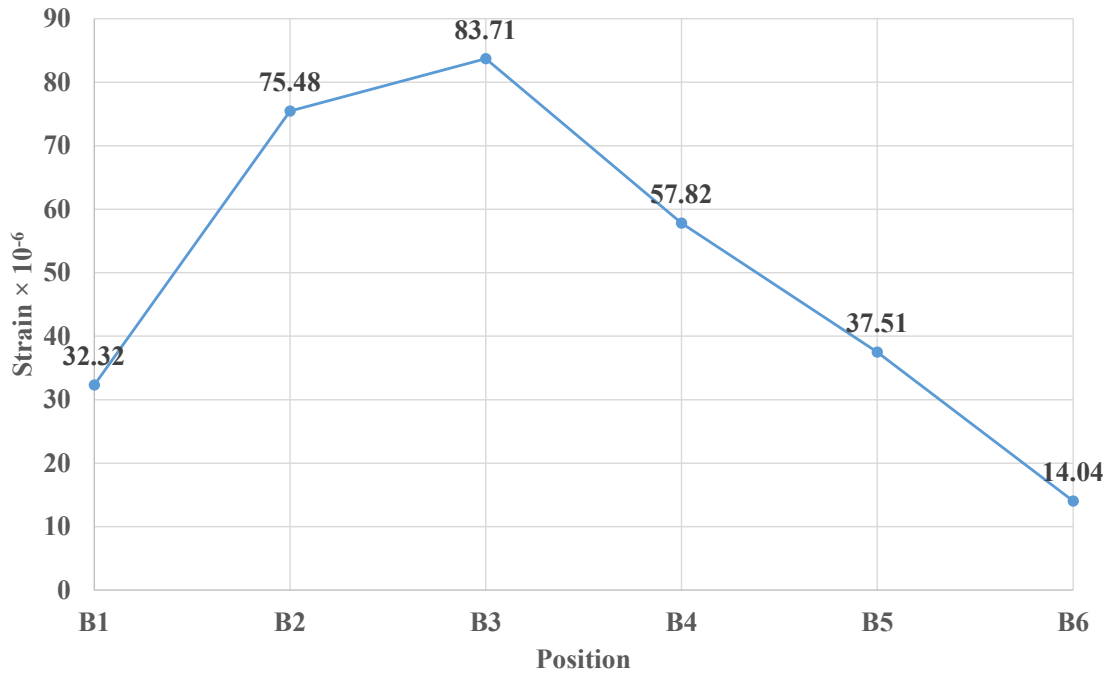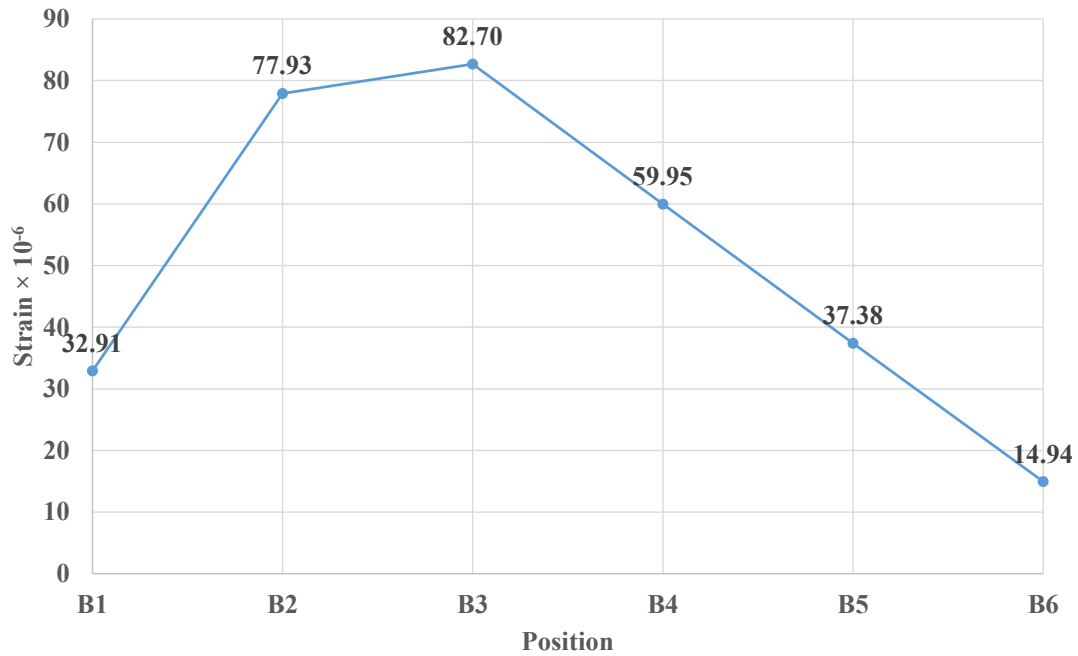**Fig. G1.** Load case 1-1 strain distribution

Fig. G2. Load case 1-1Re strain distribution

Fig. G3. Load case 2-1 strain distribution
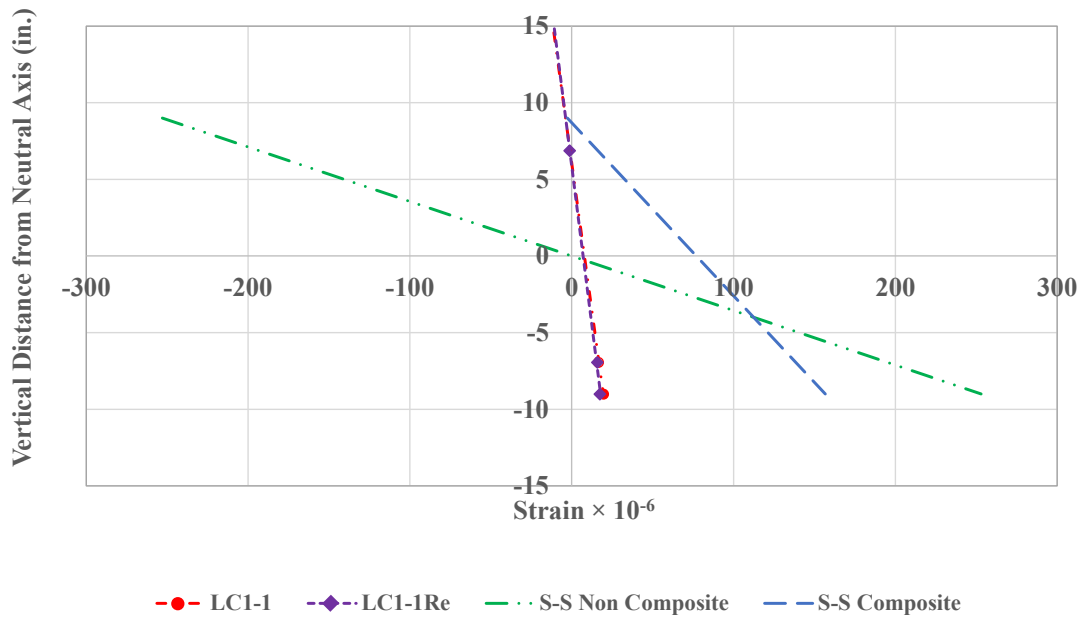

Fig. G4. Load case 2-2 strain distribution

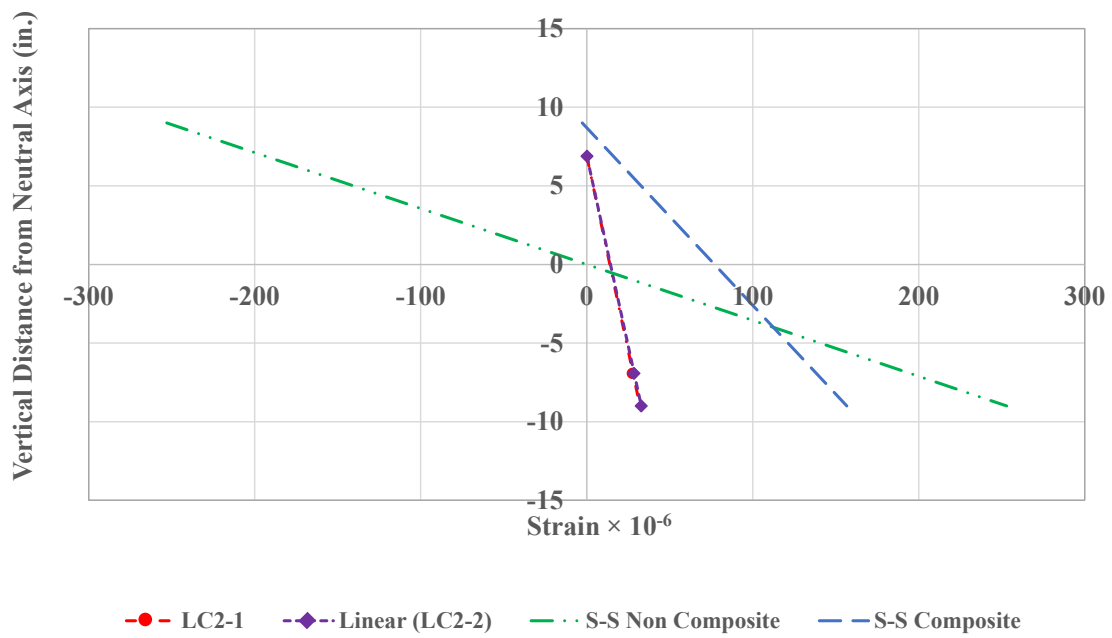Fig. G5. B1 strain profile - load case 1

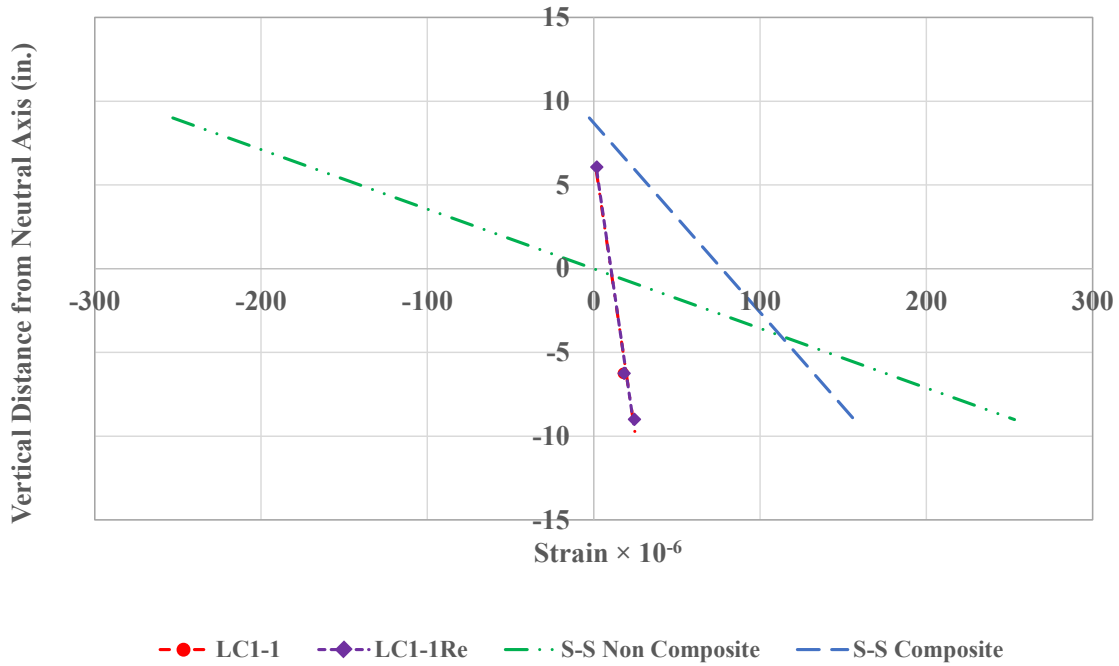Fig. G6. B1 strain profile – load case 2

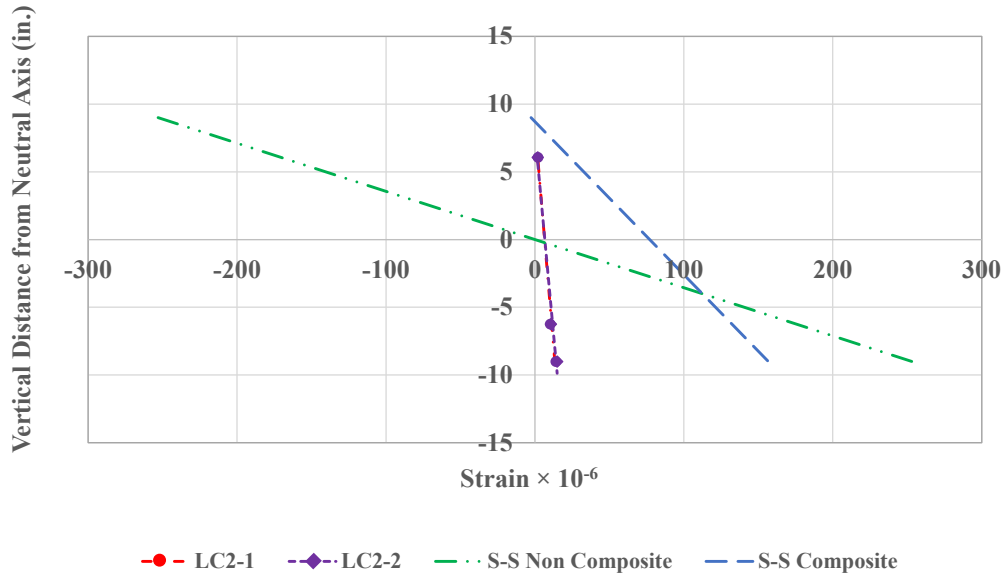**Fig.** G7**.** B6 strain profile – load case 1

Fig. G8**.** B6 strain profile – load case 2

Appendix H. Load Rating Through Load Test Results For Hardin Co. Bridge

Field load test Distribution Factor:

$$DF = \sum (\varepsilon_{interior\ beam}/\varepsilon_{all\ beams})$$
$$= 94.6 / (69.1+94.6+79.5+32.7+18.3+6.5)$$
$$= 0.315$$

Live load Moment of Test Truck:

Load per beam $P_1 = 27.92$ kips (rear axle weight at mid span)
$$M_{L1} = 172.2 \text{ kip-ft}$$

$$M_L = (172.2) \times 0.315 = 54.2 \text{ kip-ft}$$

The maximum strain due to M_L:

$$\varepsilon_c = M_L/(E \times S_x)$$
$$= 54.2 \times 12 /(29{,}000 \times 88.9)$$
$$= 252 \text{ microstrains}$$

$$\varepsilon_T = 98.95 \text{ microstrains (from field test readings)}$$

Therefore from NCHRP *Manual for Bridge Rating through Load Testing* Eq. (6-4)

$$K_a = (\varepsilon_c/\varepsilon_T) - 1$$
$$= (252/98.95) - 1 = 1.55$$

From NCHRP *Manual for Bridge Rating through Load Testing* Eq. (6-6)

$$K_b = K_{b1} \times K_{b2} \times K_{b3}$$
$$= 0.8 \times 0.8 \times 1 = 0.64 \text{ (HS20, KY1, KY2, KY3)}$$
$$= 1.0 \times 0.8 \times 1 = 0.8 \text{ (KY4)}$$

From NCHRP *Manual for Bridge Rating through Load Testing* Eq. (6-3)

$$K = 1 + K_a \times K_b$$
$$= 1 + (1.55 \times 0.64) = 1.99 \text{ (HS20, KY1, KY2, KY3)}$$
$$= 1 + (1.55 \times 0.8) = 2.24 \text{ (KY4)}$$

Truck Type HS20 (from calculations in Appendix B)
Inventory level RF = 0.916
Operating level RF = 1.529

From NCHRP *Manual for Bridge Rating through Load Testing* Eq. (6-1)
$$RF_T = RF \times K$$

Inventory level RF_T = 0.916 × 1.99 = 1.83
Operating level RF_T = 1.529 × 1.99 = 3.05